

1 **Mechanisms of *Trichodesmium* demise within the New**  
2 **Caledonian lagoon during the VAHINE mesocosm**  
3 **experiment**

4

5 **Dina Spungin<sup>1</sup>, Ulrike Pfreundt<sup>2</sup>, Hugo Berthelot<sup>3</sup>, Sophie Bonnet<sup>3,4</sup>, Dina**  
6 **AlRoumi<sup>5</sup>, Frank Natale<sup>5</sup>, Wolfgang R. Hess<sup>2</sup>, Kay D. Bidle<sup>5</sup>, Ilana Berman-Frank<sup>1</sup>**

7

8 [1] {The Mina and Everard Goodman Faculty of Life Sciences, Bar-Ilan University, Ramat-  
9 Gan, Israel}

10 [2] {University of Freiburg, Faculty of Biology, Schänzlestr. 1, D-79104 Freiburg, Germany}

11 [3] {Aix Marseille Université, CNRS/INSU, Université de Toulon, IRD, Mediterranean  
12 Institute of Oceanography (MIO) UM 110, 13288, Marseille, France}

13 [4] {Institut de Recherche pour le Développement (IRD), AMU/CNRS/INSU, Université de  
14 Toulon, Mediterranean Institute of Oceanography (MIO) UM 110, 13288, Marseille-Noumea,  
15 France-New Caledonia}

16 [5] {Department of Marine and Coastal Sciences, Rutgers University, New Brunswick, NJ,  
17 USA}

18

19 Correspondence to: I. Berman-Frank (ilana.berman-frank@biu.ac.il)

20

21

22

23

24 **Abstract**

25 The globally important marine diazotrophic cyanobacterium *Trichodesmium* is abundant in the  
26 New Caledonian lagoon (Southwestern Pacific ocean) during austral spring/summer. We  
27 investigated the cellular processes mediating *Trichodesmium* mortality from large surface  
28 accumulations (blooms) in the lagoon. *Trichodesmium* cells (and associated microbiota) were  
29 collected at the time of surface accumulation, enclosed under simulated ambient conditions,  
30 and sampled over time to elucidate the stressors and subcellular underpinning of rapid biomass  
31 demise (> 90 % biomass crashed within ~ 24 h). Metatranscriptomic profiling of  
32 *Trichodesmium* biomass, 8 h and 22 h after incubations of surface accumulations,  
33 demonstrated upregulated expression of genes required to increase phosphorus (P) and iron  
34 (Fe) availability and transport while genes responsible for nutrient storage were  
35 downregulated. Total viral abundance, oscillated throughout the experiment and showed no  
36 significant relationship with the development or demise of the *Trichodesmium* biomass.  
37 Enhanced caspase-specific activity and upregulated expression of a suite of metacaspase  
38 genes, as the *Trichodesmium* biomass crashed, implicated autocatalytic programmed cell death  
39 (PCD) as the mechanistic cause. Concurrently, genes associated with buoyancy and gas-  
40 vesicle production were strongly downregulated concomitant with increased production and  
41 high concentrations of transparent exopolymeric particles (TEP). The rapid, PCD-mediated,  
42 decline of the *Trichodesmium* biomass, as we observed from our incubations, parallels  
43 mortality rates reported from *Trichodesmium* blooms *in situ*. Our results suggest that,  
44 whatever the ultimate factor, PCD-mediated death in *Trichodesmium* can rapidly terminate  
45 blooms, facilitate aggregation, and expedite vertical flux to depth.

46

47

48

49

50

51

52

53

## 54 **1 Introduction**

55 The filamentous N<sub>2</sub>-fixing (diazotrophic) cyanobacteria *Trichodesmium* spp. are important  
56 contributors to marine N<sub>2</sub> fixation as they form massive blooms (surface accumulations with  
57 high biomass density) throughout the oligotrophic marine sub-tropical and tropical oceans  
58 (Capone et al., 2004; Capone and Carpenter, 1982; Capone et al., 1997). These surface blooms  
59 with densities of 3000 to > 10,000 trichomes L<sup>-1</sup> and chlorophyll *a* (Chl *a*) concentrations  
60 ranging from 1-5 mg L<sup>-1</sup> develop swiftly and are characterized by high rates of CO<sub>2</sub> and N<sub>2</sub>  
61 fixation (Capone et al., 1998; Luo et al., 2012; Rodier and Le Borgne, 2008; Rodier and Le  
62 Borgne, 2010). *Trichodesmium* blooms also occur frequently during austral summer between  
63 November and March over large areas of the New Caledonian lagoon in the Southwest Pacific  
64 Ocean (Dandonneau and Gohin, 1984; Dupouy et al., 2011).

65 *Trichodesmium* has been extensively investigated [reviewed in Capone et al. (1997); and  
66 Bergman et al. (2012)]. Yet, relatively few publications have examined the mortality and fate  
67 of these blooms that often collapse abruptly with mortality rates paralleling growth rates and  
68 biomass declines > 50 % occurring within 24 h from peak abundance (Bergman et al., 2012;  
69 Rodier and Le Borgne, 2008; Rodier and Le Borgne, 2010). Cell mortality can occur due to  
70 grazing of *Trichodesmium* by pelagic harpacticoid copepods (O'Neil, 1998) or by viral lysis  
71 (Hewson et al., 2004; Ohki, 1999). Both iron (Fe) and phosphorus (P) availability regulate N<sub>2</sub>  
72 fixation and production of *Trichodesmium* populations, causing a variety of stress responses  
73 when these nutrients are limited (Berman-Frank et al., 2001). Fe depletion as well as oxidative  
74 stress can also induce in *Trichodesmium* a genetically controlled programmed cell death  
75 (PCD) that occurs in both laboratory cultures and in natural populations (Bar-Zeev et al.,  
76 2013; Berman-Frank et al., 2004; Berman-Frank et al., 2007). Mortality of *Trichodesmium* via  
77 PCD is morphologically and physiologically distinct from necrotic death and triggers rapid  
78 sinking of biomass that could enhance carbon export in oligotrophic environments (Bar-Zeev  
79 et al., 2013). Sinking is due to concomitant internal cellular degradation, vacuole loss, and the  
80 increased production of extracellular polysaccharide aggregates, operationally defined as  
81 transparent exopolymeric particles (TEP) (Bar-Zeev et al., 2013; Berman-Frank et al., 2004;  
82 Berman-Frank et al., 2007).

83 The VAHINE project investigated the fate of newly fixed N by diazotrophs and aimed to test  
84 changes in organic matter export, following diazotroph development and mortality. For this,  
85 large (50 m<sup>3</sup>) mesocosms were deployed in the in the New Caledonian lagoon and followed  
86 over the course of 23 days (Bonnet et al., 2016a). Our objective during the VAHINE project

87 was to study the involvement of PCD in the fate of natural *Trichodesmium* blooms induced in  
88 these mesocosms. While *Trichodesmium* was initially present, and conditions in the  
89 mesocosms appeared favorable, no *Trichodesmium* blooms developed within the mesocosms,  
90 yet UCYN-C did increase, allowing to meet the scientific objectives of the project (Berthelot  
91 et al., 2015; Bonnet et al., 2016a; Turk-Kubo et al., 2015). However, *Trichodesmium*  
92 developed at different phases of the experimental period outside the mesocosms (Turk-Kubo  
93 et al., 2015). Here, we investigated mortality processes in a short-lived *Trichodesmium* bloom  
94 that developed and crashed in the lagoon waters at the end of the VAHINE experiment. Using  
95 a series of microcosm incubations with collected *Trichodesmium* biomass, we elucidated the  
96 stressors and subcellular underpinning of rapid (~ 24 h) biomass demise and disappearance.  
97 Here we present, for the first time, physiological, biochemical, and metatranscriptomic  
98 evidence for nutrient-stress induced PCD in natural populations that lead to *Trichodesmium*  
99 mortality including concomitant downregulation of gas vesicle synthesis and enhanced TEP  
100 production. Such mechanisms would lead to enhanced export flux in natural blooms that also  
101 crash within 1-2 days.

102

## 103 **2 Methods**

### 104 **2.1. Sampling site and sampling conditions during pre-bloom periods**

105 Our study was performed during the VAHINE mesocosm project set 28 km off the coast of  
106 New Caledonia from 13 January 2013 (day 1) to 6 February 2013 in the New Caledonian  
107 oligotrophic lagoon (22°29.10' S, 166° 26.90' E). The 25 m deep sandy-bottom lagoon is  
108 generally protected from the dominant trade winds yet the waters of the lagoon are influenced  
109 by the oligotrophic oceanic waters coming into the lagoon via the Boulari Pass (Bonnet et al.,  
110 2016a). Detailed descriptions of the site selection and sampling strategy are provided  
111 elsewhere (Bonnet et al., 2016a). The lagoon water outside the mesocosms was sampled daily  
112 during the experiment and served as the source for 'pre-bloom' data. Large volume samples  
113 (50 L) were collected from 1, 6, and 12 m depths at 07:00 using a Teflon® PFA pump and  
114 PVC tubing. Samples were immediately transferred back to laboratories aboard the R/V Alis  
115 and subsampled for a suite of parameters [as described below and in Bonnet et al. (2016a)].  
116 On day 23 at 12:00 h, we observed a large surface accumulation of *Trichodesmium* in the  
117 lagoon close to the enclosed mesocosms. This biomass accumulation (hereafter called –  
118 “bloom”) served as the source for experiments 1 and 2 to examine the fate of *Trichodesmium*  
119 (section 2.2, Fig. S1).

## 120 **2.2. Short-term incubations to assess bloom decline**

121 **Experiment 1** – *Trichodesmium* filaments and colonies were collected from the dense surface  
122 bloom (day 23, 12:00 h; designated T<sub>0</sub>, Fig. 2a-c) using a plankton net (mesh size, 80 μm)  
123 towed through different patches of the bloom from the surface water. The total contents of the  
124 net were combined and resuspended in filtered seawater (FSW) (0.2 μm pore size), split  
125 between six identical 4.5 L Nalgene polycarbonate bottles (Fig. 2d-e), and incubated as  
126 detailed below. Based on previous experience (Berman-Frank et al., 2004), resuspension of  
127 *Trichodesmium* cells in the extremely high densities of the surface blooms (> 1 mg L<sup>-1</sup> Chl *a*;  
128 Fig. 2a-c) would cause an almost immediate crash of the biomass. Consequently, we  
129 resuspended the collected biomass in FSW at ~ 1000 fold lower cell densities (150 μg L<sup>-1</sup>) that  
130 resemble the cellular abundance at the edges of the slicks (Fig. 2). **Experiment 2** – Seawater  
131 from the surface bloom was collected 5 h after the initial surface bloom was sighted (day 23,  
132 17:00) by using a Teflon® PFA pump and PVC tubing directly filling nine 20 L polyethylene  
133 carboys gently to avoid destroying biomass. Bottles from experiments 1 and 2 were placed in  
134 on-deck incubators, filled with running seawater to maintain ambient surface temperature (~  
135 26 °C), and covered with neutral screening at 50 % surface irradiance levels. Water from  
136 experiment 1 was sampled every 2-4 h until the biomass collapsed (after ~ 22 h) for: Chl *a*  
137 concentration, caspase activity, 16S rRNA gene sequencing, and metatranscriptomics. Water  
138 from experiment 2 was sampled for PON, POC, NH<sub>4</sub><sup>+</sup>, N<sub>2</sub> fixation rates, TEP production, and  
139 virus abundance (days 23-25) (Fig. S1). Prior to incubations, all incubation bottles and  
140 carboys were washed with 10 % HCl overnight and rinsed 3 times with ambient seawater.

## 141 **2.3. Chlorophyll *a* concentrations**

142 Samples for the determination of Chl *a* concentrations during pre-bloom days were collected  
143 by filtering 550 mL of seawater on GF/F filters. Filters were directly stored in liquid nitrogen.  
144 Chl *a* was extracted in methanol and measured fluorometrically (Herbland et al., 1985).  
145 During short-term experiment 1, samples for Chl *a* were collected by filtering 200 mL on  
146 GF/F filters (Whatman, Kent, UK). Chl *a* was extracted in methanol and measured  
147 spectrophotometrically (664 and 750 nm; CARY100, Varian, Santa Clara, CA, USA)  
148 according to Tandeau de Marsac and Houmard (1988).

149

150

## 151 **2.4. Particulate organic carbon (POC) and nitrogen (PON)**

152 Detailed POC and PON analyses are described in Berthelot et al. (2015). POC samples were  
153 collected by filtering 2.3 L of seawater through pre-combusted (450 °C, 4 h) GF/F filter and  
154 determined using the combustion method (Strickland and Parsons, 1972) on an EA 2400 CHN  
155 analyzer. Samples for PON concentrations were collected by filtering 1.2 L of water on pre-  
156 combusted (450 °C, 4 h) and acid washed (HCl, 10 %) GF/F filters and analyzed according to  
157 the wet oxidation protocol described in Pujo-Pay and Raimbault (1994) with a precision of  
158 0.06  $\mu\text{mol L}^{-1}$ .

## 159 **2.5. N<sub>2</sub> fixation rates and NH<sub>4</sub><sup>+</sup> concentrations**

160 N<sub>2</sub>-fixation rate measurements used in experiment 2 are described in detail in (Berthelot et al.,  
161 2015). Samples were collected at 17:00 in 4.5 L polycarbonate bottles and amended with <sup>15</sup>N<sub>2</sub>-  
162 enriched seawater, within an hour of biomass collection, according to the protocol developed  
163 by Mohr et al. (2010) and Rahav et al. (2013). Briefly, seawater was degassed through a  
164 degassing membrane (Membrana, Minimodule®, flow rate fixed at 450 mL min<sup>-1</sup>) connected  
165 to a vacuum pump. Degassed seawater was amended with 1 mL of <sup>15</sup>N<sub>2</sub> (98.9 % atom <sup>15</sup>N,  
166 Cambridge Isotopes) per 100 mL. The bottle was shaken vigorously and incubated overnight  
167 at 3 bars to promote <sup>15</sup>N<sub>2</sub> dissolution. Incubation bottles were amended with 1:20 (vol:vol) of  
168 <sup>15</sup>N<sub>2</sub>-enriched seawater, closed without headspace with silicone septum caps, and incubated  
169 for 24 h under *in situ*-simulated conditions in on-deck incubators (described above). 2.2 L  
170 from each experimental bottle was filtered under low vacuum pressure (< 100 mm Hg) onto a  
171 pre-combusted (450 °C, 4 h) GF/F filter (25 mm diameter, 0.7  $\mu\text{m}$  nominal porosity). The  
172 filters were stored at -20 °C and dried for 24 h at 60 °C before mass spectrometric analysis.  
173 PON content and PON <sup>15</sup>N enrichments were determined using a Delta plus Thermo Fisher  
174 Scientific isotope ratio mass spectrometer (Bremen, Germany) coupled with an elemental  
175 analyzer (Flash EA, Thermo Fisher Scientific). N<sub>2</sub>-fixation rates were calculated according to  
176 the equations detailed in Montoya et al. (1996). We assumed significant rates when the <sup>15</sup>N  
177 enrichment of the PON was higher than three times the standard deviation obtained from T<sub>0</sub>  
178 samples. The <sup>15</sup>N batch did not indicate that our results were overestimated by contamination  
179 of the spike solution (Berthelot et al. 2015).

180 Samples for NH<sub>4</sub><sup>+</sup> were collected in 40 mL glass vials and analyzed by the fluorescence  
181 method according to Holmes et al. (1999), using a Trilogy fluorometer (Turner Design).

182

183 **2.6. Transparent exopolymeric particles (TEP)**

184 Water samples (100 mL) were gently (< 150 mbar) filtered through 0.45 µm polycarbonate  
185 filter (GE Water & Process Technologies). Filters were then stained with a solution of 0.02 %  
186 Alcian blue (AB), 0.06 % acetic acid (pH of 2.5), and the excess dye was removed by a quick  
187 deionized water rinse. Filters were then immersed in sulfuric acid (80 %) for 2 h, and the  
188 absorbance (787 nm) was measured spectrophotometrically (CARY 100, Varian). AB was  
189 calibrated using a purified polysaccharide gum xanthan (GX) (Passow and Alldredge, 1995).  
190 TEP concentrations (µg GX equivalents L<sup>-1</sup>) were measured according to (Passow and  
191 Alldredge, 1995).

192

193 **2.7. Virus abundance**

194 Total seawater (1 mL) was fixed with 0.5 % glutaraldehyde and snap frozen in liquid N<sub>2</sub> until  
195 processed. Flow cytometry was conducted using an Influx Model 209S Mariner flow  
196 cytometer and high-speed cell sorter equipped with a 488 nm 200 mW blue laser, 4 way sort  
197 module, 2 scatter, 2 polarized and 4 fluorescence detectors (BD Biosciences). Viral abundance  
198 was determined by staining fixed seawater samples with SYBR Gold (Life Technologies) and  
199 measurements of green fluorescence (520 nm, 40 nm band pass). Samples were thawed,  
200 diluted 25-fold in 0.22 µm-filtered Tris/EDTA (TE) buffer (pH 8), stained with SYBR Gold  
201 (0.5 - 1X final concentration), incubated for 10 min at 80°C in the dark, cooled to RT for 5  
202 min, and mixed thoroughly by vortexing prior to counting on the Influx (Brussaard, 2003).  
203 Viral abundance was analyzed using a pressure differential (between sheath and sample fluid)  
204 of 0.7, resulting in a low flow rate for higher event rates of virus like particles counts.

205 **2.8. Caspase activity**

206 Biomass was collected on 25 mm, 5 µm pore-size polycarbonate filters and resuspended in  
207 0.6-1 mL Lauber buffer [50 mM HEPES (pH 7.3), 100 mM NaCl, 10 % sucrose, 0.1 % 3-(3-  
208 cholamidopropyl)-dimethylammonio-1-propanesulfonate, and 10 mM dithiothreitol] and  
209 sonicated on ice (four cycles of 30 seconds each) using an ultra-cell disruptor (Sonic  
210 Dismembrator, Fisher Scientific, Waltham, MA, USA). Cell extracts were centrifuged (10,000  
211 x g, 2 min, room temperature) and supernatant was collected for caspase biochemical activity.  
212 Caspase-specific activity was determined by measuring the kinetics of cleavage for the  
213 canonical fluorogenic caspase substrate (Z-IETD-AFC) at a 50 mM final concentration (using  
214 Ex 400 nm and emission 505 nm; Synergy4 BioTek, Winooski, VT, USA), as previously  
215 described in Bar-Zeev et al. (2013). Fluorescence was converted to a normalized substrate

216 cleavage rate using an AFC standard (Sigma) and normalized to total protein concentrations  
217 obtained from the same samples. Total protein concentrations were determined by Pierce™  
218 BCA Protein Assay Kit (Thermo Scientific product #23225).

## 219 **2.9. 16S rRNA gene sequencing and data analyses**

220 Bacterial community diversity was analyzed by deep sequencing of the 16S rRNA gene in  
221 samples from two replicate bottles from experiment 1 (see section 1.2) at three time points  
222 each. Seawater samples were filtered on 25 mm, 5 µm pore-size Supor filters (Pall Gelman  
223 Inc., Ann Arbor, Michigan), snap frozen in liquid nitrogen, and stored at -80 °C for later  
224 extraction. Community genomic DNA was isolated from the filters using a phenol–chloroform  
225 extraction method modified according to Massana et al. (1997). The 16S rRNA genes within  
226 community genomic DNA were initially amplified with conserved bacterial primers 27F and  
227 1100R (Dowd et al., 2008) using a high fidelity polymerase (Phusion DNA polymerase,  
228 Thermo Scientific) with an initial denaturation step of 95 °C for 3 min followed by 20 cycles  
229 of 95 °C for 30 sec, 55 °C for 30 sec, and 72 °C for 45 sec. A secondary PCR (same  
230 conditions) was performed for next-generation sequencing by using customized fusion primers  
231 with different tag sequences. The tags were attached to the 27F primer and to the 338R primer  
232 (Hamady et al., 2008) to obtain 340 bp fragments suitable for IonTorrent analysis. The use of  
233 nested PCR was used to minimize inclusion of false sequences into the sequenced material  
234 (Dowd et al., 2008). After secondary PCR, all amplicon products were purified using Ampure  
235 magnetic purification beads (Agencourt Bio- science Corporation, MA, USA) to exclude  
236 primer-dimers. The amplicons were sequenced at the Bar-Ilan Sequencing Center, using an  
237 Ion Torrent™ (Life Technologies, USA).

238 The adapter-clipped sequences were processed using tools and scripts from the UPARSE  
239 pipeline (Edgar, 2013). Reads from all samples were pooled for OTU calling. Reads were de-  
240 multiplexed, primers and barcodes stripped using the script *fastq\_strip\_barcode\_relabel.py*,  
241 leaving 42747 raw reads altogether for six samples. As suggested for OTU calling from  
242 single-end amplicon sequences (Edgar, 2013), sequences (mostly between 280 nt and 300 nt)  
243 were trimmed to a fixed length of 280 nt, and shorter sequences were discarded (26740  
244 trimmed raw reads remaining). For OTU clustering, trimmed raw reads were quality filtered  
245 using the *-fastq\_filter* command with a maximum expected error rate (*-fastq\_maxee*) of 2  
246 (21590 reads remaining), clustered into unicals (100 % identity) and the unicals sorted by  
247 weight (number of sequences in the cluster). OTU clustering with an identity threshold of 0.98



248 was done using the *-cluster\_otus* command on sorted unicals, with built-in chimera filtering.  
249 To infer OTU abundances for each individual sample, the trimmed raw reads per sample (after  
250 a more relaxed quality filtering with *-fastq\_maxee* 5) were mapped back to these OTUs with *-*  
251 *usearch\_global* and a minimum identity of 98 %. For taxonomic classification, OTUs were  
252 submitted to <https://www.arb-silva.de/ngs/> and classified using the SINA aligner v1.2.10 and  
253 database release SSU 123 (Quast et al., 2013). Sequences having a  $(BLAST\ alignment\ coverage + alignment\ identity)/2 < 93\ %$  were considered as unclassified and assigned to the  
254 virtual group “No Relative” (5.58 % of OTUs).  
255

## 256 **2.10. RNA extraction and metatranscriptome sequencing**

257 Metatranscriptomic sequencing was performed for three time points: peak surface  
258 accumulation of the bloom (T<sub>0</sub>, 12:00), 8 h (T<sub>8</sub> 22:00), and 22 h (T<sub>22</sub> 10:00) after T<sub>0</sub>. Cells on  
259 polycarbonate filters were resuspended in 1 mL PGTX [for 100 mL final volume: phenol  
260 (39.6 g), glycerol (6.9 mL), 8-hydroxyquinoline (0.1 g), EDTA (0.58 g), sodium acetate (0.8  
261 g), guanidine thiocyanate (9.5 g), guanidine hydrochloride (4.6 g), Triton X-100 (2 mL)]  
262 (Pinto et al., 2009), and 250 µl glass beads (diameter 0.1 – 0.25 mm). and sonicated on a cell  
263 disruptor (Precellys, Peqlab, Germany) for 3 x 15 s at 6500 rpm. Tubes were placed on ice  
264 between each 15 s interval. RNA was extracted by adding 0.7 mL chloroform and subsequent  
265 phase separation. RNA was precipitated from the aqueous phase using 3 volumes of  
266 isopropanol at -20 °C overnight. Residual DNA was removed using the Turbo DNA-free Kit  
267 (Ambion) after the manufacturer’s instructions, but adding additional 1 µl of DNase after 30  
268 min of incubation and incubating another 30 min. RNA was purified using Clean &  
269 Concentrator 5 columns (C&C 5) (Zymo Research, Freiburg, Germany). The pure RNA was  
270 treated with Ribo-Zero rRNA Removal Kit (Bacteria) (Epicentre, Madison, USA) and  
271 purified again with C&C 5. DNA contamination was tested and confirmed negative with a 40  
272 cycle PCR using cyanobacteria-specific 16S primers.

273 For removal of tRNAs and small fragments, the RNA was purified with the Agencourt  
274 RNAClean XP kit (Beckman Coulter Genomics, Danvers, USA). First-strand cDNA synthesis  
275 for T<sub>8</sub> and T<sub>22</sub> samples was primed with a N6 randomized primer, after which the cDNAs were  
276 fragmented by ultrasound (4 pulses of 30 sec at 4 °C). Illumina TruSeq sequencing adapters  
277 were ligated in a strand-specific way to the 5' and 3' ends and the resulting cDNAs were PCR-  
278 amplified to about 10-20 ng µL<sup>-1</sup> using a high fidelity DNA polymerase. Randomly-primed  
279 cDNA for T<sub>0</sub> samples was prepared using purified RNA without fragmentation followed by

280 ligation of Illumina TruSeq sequencing adapters to the 5' and 3' ends and fragmentation of  
281 cDNA > ~700 bp with ultrasound (4 pulses of 30 sec at 4°C; targeting only cDNA > 700 nt).  
282 After repairing ends, fragments were dA-tailed and Illumina TruSeq sequencing adapters were  
283 ligated again to the 5' and 3' ends of the cDNA and re-amplified. Consequently, a small  
284 fraction of the T<sub>0</sub> reads was not strand-specific. All cDNAs were purified using the Agencourt  
285 AMPure XP kit (Beckman Coulter Genomics, Danvers, USA) and 2 x 150 nt paired-end  
286 sequences generated with an Illumina NextSeq500 sequencer by a commercial provider (vertis  
287 AG, Freising, Germany).

## 288 **2.11. Bioinformatics processing and analysis of metatranscriptome data**

289 To remove adapters, perform quality trimming, and set a minimal length cutoff, raw fastq  
290 reads were processed with Cutadapt version 1.8.1 (Martin, 2011) in paired-end mode with a  
291 minimum adapter sequence overlap of 10 nt (-O 10), an allowed error rate of 20 % (-e 0.2) in  
292 the adapter sequence alignment, and a minimum base quality of 20. To remove residual  
293 ribosomal RNA reads, the fastq files were further processed with SortMeRNA version 1.8  
294 (Kopylova et al., 2012) with the accompanying standard databases in paired end mode,  
295 resulting in 9,469,339 non-ribosomal reads for T<sub>0</sub>, 22,407,194 for T<sub>8</sub>, and 18,550,250 for T<sub>22</sub>.  
296 The fastq files with all non-ribosomal forward-reads were used for mapping against the  
297 *Trichodesmium erythraeum* IMS101 genome with Bowtie2 (Langmead and Salzberg, 2012) in  
298 *very-sensitive-local* mode. This resulted in 51.9 % of T<sub>0</sub>, 5.1 % of T<sub>8</sub>, and 3.3 % of T<sub>22</sub> reads  
299 mapped. Reads were counted per CDS feature as annotated in the genome of *Trichodesmium*  
300 *erythraeum* (NC\_008312.1) using htseq-count version 0.6.0 (Anders et al., 2014) and a count  
301 table generated with all read counts from T<sub>0</sub>, T<sub>8</sub>, and T<sub>22</sub>.

302 For detection of differentially expressed genes from T<sub>0</sub> to T<sub>8</sub> and T<sub>8</sub> to T<sub>22</sub>, the count table was  
303 processed with the statistical tool “Analysis of Sequence Counts” (ASC) (Wu et al., 2010).  
304 This tool is specifically designed to account for missing replicates by employing a model of  
305 biological variation of gene expression (Wu et al., 2010). The posterior probabilities (P) of a  
306 gene being > 2-fold differentially expressed (user specified threshold) between any two  
307 samples is calculated using an empirical Bayesian analysis algorithm and an internal  
308 normalization step. Differential expression of genes was defined as significant if P > 0.98.

309

310

### 311 3 Results

#### 312 3.1. Setting the scene – *Trichodesmium* bloom development and bloom within 313 the lagoon.

314 *Trichodesmium* were present as part of the *in-situ* community in the lagoon at the outset of the  
315 VAHINE experiment. (Bonnet et al., 2015; Turk-Kubo et al., 2015). In the lagoon water,  
316 temperatures were high (> 25 °C) and typical oligotrophic conditions of austral summer  
317 prevailed. For the first 20 days of the experiment low abundance and biomass was measured  
318 for primary and secondary production and specifically for diazotrophic populations (Fig. 1).  
319 Total PON and POC in the lagoon fluctuated in the first 20 days of the VAHINE experiment  
320 with values ranging between 0.6-1.1  $\mu\text{mol L}^{-1}$  and 5-11 respectively. On the morning of day  
321 23, values were 0.9 and 9.3  $\mu\text{mol L}^{-1}$  PON and POC, respectively (Fig. 1c-d). The total Chl *a*  
322 concentrations ranged between 0.18-0.26  $\mu\text{g L}^{-1}$  from days 1-20 (Fig. 1a). The increase in Chl  
323 *a* concentrations reflect the composite signature of the total phototrophic community [detailed  
324 in (Leblanc et al., 2016; Van Wambeke et al., 2015)] and is not specific to *Trichodesmium*  
325 biomass. Low abundances of *Trichodesmium* were measured in the lagoon waters throughout  
326 the first three weeks of the project (Turk-Kubo et al., 2015), with *Trichodesmium*-associated  
327 16S counts ranging from 0.1 to 0.4 % of the total number of 16S tags (Pfreundt et al., 2016).  
328 During the first eight days of sampling, *Trichodesmium* abundance as measured by *nifH* gene  
329 real-time PCR ranged from  $3.4 \times 10^2$ - $6.5 \times 10^3$  *nifH* copies  $\text{L}^{-1}$ . By days 14 and 16,  
330 *Trichodesmium* accounted for 15 % of the total diazotroph population (with  $1.1$ - $1.5 \times 10^4$  *nifH*  
331 copies  $\text{L}^{-1}$ ) increasing by day 22 to 42 % of the diazotroph population ( $1.4 \times 10^5$  *nifH* copies  $\text{L}^{-1}$ )  
332 (Turk-Kubo et al., 2015). By the morning of day 23, Chl *a* increased to 0.39  $\mu\text{g L}^{-1}$  in the  
333 upper 1 m depth (Fig. 1a), yet *Trichodesmium* was still not visually observed at this time as a  
334 bloom on the sea surface. Phycoerythrin concentrations fluctuated between 0.1-0.4  $\mu\text{g L}^{-1}$   
335 during days 1-14 and then increased to a maximal peak of > 0.8  $\mu\text{g L}^{-1}$  on day 21 with values  
336 ~ 0.5  $\mu\text{g L}^{-1}$  on day 23 reflecting both the doubling in *Synechococcus* biomass (days 15-23) as  
337 well as increasing *Trichodesmium* (days 21-23) (Leblanc et al., 2016).  $\text{N}_2$  fixation rates in the  
338 lagoon waters ranged between 0.09 -1.2  $\text{nmol N L}^{-1} \text{h}^{-1}$  during the pre-bloom period (Fig. 1c)  
339 and on the morning of day 23 measured 0.5  $\text{nmol L}^{-1} \text{h}^{-1}$  (Fig. 1c).

340 Zooplankton populations in the lagoon fluctuated around 5000 individuals  $\text{m}^{-3}$  and increased  
341 from day 9 to 16 to peak at ~ 14000 individuals  $\text{m}^{-3}$  (Hunt et al., 2016). From day 16 to day 23  
342 the total zooplankton population declined to ~ 8000 individuals  $\text{m}^{-3}$  with harpacticoid  
343 copepods including grazers of *Trichodesmium* (*Macrosetella gracilis*, *Miracia efferata*, and  
344 *Oculosetella gracilis*) comprising < 1.5 % of total zooplankton community in the lagoon

345 (Hunt et al., 2016). Virus like particles (VLP) ranged from  $1-6 \times 10^6 \text{ mL}^{-1}$  throughout the first  
346 22 days of the VAHINE experiment and displayed a  $\sim 2-4$  day oscillation (i.e., increasing for  
347 2 days, then declining for the next 3 days, etc.) with mean values of  $3.8 \times 10^6 \text{ mL}^{-1}$  (Fig. 1b).  
348 VLP counts in surface waters on day 23 were  $1.8 \times 10^6 \text{ mL}^{-1}$  (Fig. 1b), just prior to the  
349 appearance of the *Trichodesmium* surface bloom. VLPs did not show any distinct correlations  
350 with total biomass indices such as PON and POC during the pre-bloom sampling (Fig. 1b-d).  
351 Depth-averaged dissolved inorganic phosphorus (DIP) concentrations in the lagoon waters  
352 were low at  $0.039 \pm 0.001 \mu\text{M}$ , with a relatively stable DIP turnover time ( $T_{\text{DIP}}$ ) of  $1.8 \pm 0.7 \text{ d}$   
353 for the first 15 days, that declined to  $0.5 \pm 0.7$  by day 23 (Berthelot et al., 2015). Alkaline  
354 phosphatase activity (APA), which hydrolyzes inorganic phosphate from organic phosphorus,  
355 increased  $\sim 3$  fold, from  $1.8 \pm 0.7$  (average of days 1-4) to  $5.0 \pm 1.4 \text{ nmole L}^{-1} \text{ h}^{-1}$  (average of  
356 days 19-23) (Van Wambeke et al., 2015) demonstrating a response in metabolic activity  
357 related to P acquisition for the microbial community probably related to the decreasing  
358 availability of DIP in the lagoon waters.

359 On day 23 (February 4) of the VAHINE measurements, dense surface accumulations of  
360 *Trichodesmium* were observed at midday (12:00 h) (Fig. 2a-c). Ambient air temperatures ( $\sim$   
361  $25 \text{ }^\circ\text{C}$ ) increased to over  $26 \text{ }^\circ\text{C}$  and the winds decreased to  $< 5$  knots. These accumulations  
362 (hereafter blooms) appeared in the typical “slick” formations of dense biomass in ribbons  
363 visible on the surface seawater and spread out over tens of meters in the lagoon water outside  
364 the mesocosms (Fig. 2a-c). *Trichodesmium* abundance in these patches was extremely variable  
365 with Chl *a* concentrations exceeding  $5 \text{ mg L}^{-1}$  within dense patches and trichome abundance  $>$   
366  $10,000$  trichomes mL. These surface accumulations were visible and sampled again 5 h later  
367 (experiment 2), yet by the next morning, no such slicks or patches of dense biomass were  
368 observed or measured in the lagoon. The disappearance of the *Trichodesmium* in the lagoon  
369 water whether by drifting away, sinking to depth, or any other factor, prevented further  
370 investigation of these populations.

371

## 372 **3.2. Investigating *Trichodesmium* mortality in experimental microcosms.**

### 373 **3.2.1 Changes in *Trichodesmium* biomass and associated microbial** 374 **communities.**

375 The spatially patchy nature of *Trichodesmium* blooms in the lagoon (Fig. 2a-c), and the rapid  
376 temporal modifications in water-column abundance of filaments and colonies probably  
377 induced (primarily) by physical drivers (turbulence and wind-stress), complicate *in-situ*

378 sampling when targeting changes in specific biomass. To overcome this, we collected  
379 *Trichodesmium* populations from the surface midday bloom and examined the physiological,  
380 biochemical, and genetic changes occurring with time until the biomass crashed ~ 24 h (see  
381 methods section 2.2) (Fig. 2 and Fig. 3). In these enclosed microcosms, *Trichodesmium* 16S  
382 copies comprised > 90 % of total copies (Fig. 3) enabling the use Chl *a* to follow changes in  
383 its biomass (Fig. 2f). Maximal Chl *a* concentrations in the incubations ( $> 150 \pm 80 \mu\text{g L}^{-1}$ ;  
384  $n=6$ ) were measured at the start of the incubation soon after the biomass collection and  
385 resuspension in FSW. These *Trichodesmium* populations collapsed swiftly over the next day  
386 with Chl *a* concentrations declining to  $24 \mu\text{g L}^{-1}$  and  $11 \mu\text{g L}^{-1}$  Chl *a* after 10 and 22 h,  
387 respectively (Fig. 2f).

388 In experiment 1 we characterized the microbial community associated with the  
389 *Trichodesmium* biomass within the microcosms by 16S rRNA gene sequencing from two  
390 replicate bottles (experiment 1). At  $T_0$  94 % and 93 % of the obtained 16S tags in both  
391 replicates (Fig. 3) were of the Oscillatoriales order (phylum Cyanobacteria), with 99.9 % of  
392 these sequences classified as *Trichodesmium* spp. (Fig. 3). In both replicates, the temporal  
393 decline of *Trichodesmium* biomass coincided with an increase in *Alteromonas* 16S tags, but  
394 this development temporally lagged in replicate 1 compared to replicate 2 (Fig. 3). Six hours  
395 ( $T_6$ ) after the surface bloom was originally sampled ( $T_0$ ), over 80 % of 16S tags from replicate  
396 1 were characterized as *Trichodesmium*. 14 h after  $T_0$ , Alteromonadales and Vibrionales  
397 replaced *Trichodesmium* now constituting only 9 % of 16S tags (Fig. 3). In replicate 2,  
398 *Trichodesmium* declined by 80 % 6 h after  $T_0$ , with Alteromonadales and Flavobacteriales  
399 comprising the bulk of the biomass 18 hours after the start of incubations (Fig.3).

400 The rate of decline in *Trichodesmium* biomass within the 4.6 L microcosms paralleled that of  
401 *Trichodesmium* collected from the surface accumulations at 17:00 and incubated in 20 L  
402 carboys under ambient conditions for > 72 h (defined hereafter as experiment 2: Fig. 4). Here,  
403 *Trichodesmium* biomass decreased by > 80 % within 24 h of incubations with trichome  
404 abundance declining from  $\sim 2500$  trichomes  $\text{mL}^{-1}$  at bloom collection to  $\sim 495$  trichomes  $\text{mL}^{-1}$   
405 (Fig. 4a). No direct correlation was observed between the decline of *Trichodesmium* and viral  
406 populations. VLP abundance at the time of the surface bloom sampling was at a maximum of  
407  $8.2 \times 10^6 \text{ mL}^{-1}$  (Fig. 4a), decreasing to  $5.7 \times 10^6 \text{ mL}^{-1}$  in the next 4 h then remaining stable  
408 throughout the crash period (within the next 42 h) averaging  $\sim 5 \times 10^6 \pm 0.7 \text{ mL}^{-1}$  (Fig. 4a).

409 As *Trichodesmium* crashed in the experimental incubations, high values of  $\text{NH}_4^+$  were  
410 measured (Fig 4b). In experiment 2,  $\text{NH}_4^+$  increased exponentially from  $73 \pm 0.0004 \text{ nmol}$   
411  $\text{NH}_4^+ \text{ L}^{-1}$  when the surface bloom was collected and placed in the carboys (17:00 h) to  $1490 \pm$   
412  $686$  after 24 h and values  $> 5000 \text{ nmol L}^{-1}$  42 h after the incubation start (Fig. 3b). The high  
413 ammonia declined somewhat by the end of the experiment (after 72 h), yet was still high at  
414  $3494 \pm 834 \text{ nmol L}^{-1}$ . Concurrently with the high  $\text{NH}_4^+$  concentrations, and despite the dying  
415 *Trichodesmium*, we measured an increase  $\text{N}_2$ -fixation rates.  $\text{N}_2$ -fixation rose from  $1.5 \text{ nmol N}$   
416  $\text{L}^{-1} \text{ h}^{-1}$  at  $T_0$  to  $3.5 \pm 2.8 \text{ nmol N L}^{-1} \text{ h}^{-1}$  8 h after incubations began and  $11.7 \pm 3.4 \text{ nmol N L}^{-1}$   
417 24 h later (Fig 4b). These high values represent other diazotrophs including UCYN-types and  
418 diatom-diazotroph associations that flourished after the *Trichodesmium* biomass had declined  
419 in the carboys (Bonnet et al. 2016b; Turk-Kubo personal communication). POC and PON,  
420 representing the fraction of C and N incorporated into biomass, ranged between  $5.2\text{-}11.2 \text{ }\mu\text{mol}$   
421  $\text{C L}^{-1}$  and  $0.6\text{-}1.1 \text{ }\mu\text{mol N L}^{-1}$  during pre-bloom periods (Fig. 1b) and  $12.6 \pm 4.6 \text{ }\mu\text{mol C L}^{-1}$   
422 and  $1.3 \pm 0.5 \text{ }\mu\text{mol N L}^{-1}$  when the surface bloom was sampled (Fig. 4b-c). 24 hours after  
423 collection of bloom biomass POC increased  $\sim 6$ -fold to  $63.2 \pm 15 \text{ }\mu\text{mol C L}^{-1}$  and PON  
424 increased 10-fold to  $10 \pm 3.3 \text{ }\mu\text{mol N L}^{-1}$  (Fig. 4b-c). After 72 h, total POC was  $62 \pm 4 \text{ }\mu\text{mol C}$   
425  $\text{L}^{-1}$  (Fig. 4c) and PON increased to  $14.1 \pm 6 \text{ }\mu\text{mol N L}^{-1}$  (Fig. 4b).

426 Organic carbon in the form of TEP is secreted when *Trichodesmium* is stressed and  
427 undergoing PCD (Bar-Zeev et al., 2013; Berman-Frank et al., 2004). TEP concentrations in  
428 the lagoon waters during the pre-bloom period (first 20 days) fluctuated around  $\sim 350 \text{ }\mu\text{g gum}$   
429 xanthan (GX)  $\text{L}^{-1}$  (Fig. 1d) that increased to  $\sim 500 \text{ }\mu\text{g GX L}^{-1}$  on day 22 (Fig. 1d). During the  
430 time of biomass collection from the surface bloom TEP concentration exceeded  $700 \text{ }\mu\text{g GX L}^{-1}$   
431  $\text{L}^{-1}$  (Fig. 4c). After biomass enclosure (experiment 2) TEP concentrations declined to  $420 \pm 35$   
432  $\mu\text{g GX L}^{-1}$  and subsequently to  $180 \pm 25 \text{ }\mu\text{g GX L}^{-1}$  42 h and 72 h after  $T_0$  (Fig. 4c).

### 433 **3.2.2. Genetic responses of stressed *Trichodesmium***

434 Metatranscriptomic analyses of the *Trichodesmium* biomass were conducted in samples from  
435 experiment 1, at  $T_0$ ,  $T_8$ , and  $T_{22}$  (Fig. S1). We examined differential expression during this  
436 period by investigating a manually curated gene suite including specific pathways involved in  
437 P and Fe uptake and assimilation, PCD, or gas vesicle synthesis. Genes involved in the  
438 acquisition and transport of inorganic and organic P sources were upregulated, concomitant  
439 with biomass demise; significantly higher expression levels were evident at  $T_8$  and  $T_{22}$   
440 compared to  $T_0$  (Table S1). Abundance of alkaline phosphatase transcripts, encoded by the

441 *phoA* gene (Orchard et al., 2003), increased significantly (~ 5 fold) from T<sub>0</sub> to T<sub>22</sub> (Fig. 5a).  
442 The transcript abundance of phosphonate transporters and C-P lyase genes (*phnC*, *phnD*,  
443 *phnE*, *phnH*, *phnI*, *phnL* and *phnM*) increased significantly (5-12 fold) between T<sub>0</sub> and both T<sub>8</sub>  
444 and T<sub>22</sub> (Fig. 5a, Table S1). Of the phosphite uptake genes, only *ptxA* involved in the  
445 phosphite (reduced inorganic phosphorus compound) uptake system, and recently found to  
446 operate in *Trichodesmium* (Martínez et al., 2012; Polyviou et al., 2015) was significantly  
447 upregulated at both T<sub>8</sub> and T<sub>22</sub> compared to T<sub>0</sub> (4.5 and 7 fold change respectively). The two  
448 additional genes involved in phosphite uptake, *ptxB* and *ptxC*, did not change significantly, as  
449 *Trichodesmium* biomass crashed (Fig. 5a).

450 Fe limitation induces PCD in *Trichodesmium* (Berman-Frank et al., 2004; Berman-Frank et  
451 al., 2007) we therefore examined genetic markers of Fe stress. At the time of surface bloom  
452 sampling (experiment 1, T<sub>0</sub>), Fe stress was indicated by higher differential expression of  
453 several genes. The *isiB* gene encodes flavodoxin and serves as a common diagnostic indicator  
454 of Fe stress in *Trichodesmium*, since it may substitute for Fe-S containing ferredoxin (Bar-  
455 Zeev et al., 2013; Chappell and Webb, 2010). Transcripts of *isiB* were significantly higher at  
456 T<sub>0</sub> (3-fold) than at T<sub>8</sub> and T<sub>22</sub> (Fig. 5b, Table S1). The chlorophyll-binding protein IsiA is  
457 induced in cyanobacterial species under Fe or oxidative stress to prevent oxidative damage  
458 (Laudenbach and Straus, 1988). Here *isiA* transcripts increased 2- and 3- fold from T<sub>0</sub> to T<sub>8</sub>  
459 and T<sub>22</sub>, respectively (Fig. 5b, Table S1). The Fe transporter gene *idiA* showed a transient  
460 higher transcript accumulation only at T<sub>8</sub>. As the health of *Trichodesmium* declined,  
461 transcripts of the Fe-storage protein ferritin (*Dps*) decreased by > 70 % at T<sub>22</sub> (Fig. 5b, Table  
462 S1)

### 463 3.2.3. PCD-induced demise.

464 Our earlier work demonstrating PCD in *Trichodesmium* allowed us to utilize two independent  
465 biomarkers to investigate PCD induction during *Trichodesmium* demise, namely changes in  
466 catalytic rates of caspase-specific activity (Berman-Frank et al., 2004; Berman-Frank et al.,  
467 2007) and levels of metacaspase transcript expression (Bar-Zeev et al., 2013). When the  
468 surface bloom was sampled (experiment 1, T<sub>0</sub>), protein normalized caspase-specific activity  
469 was  $0.23 \pm 0.2$  pmol mg protein<sup>-1</sup> min<sup>-1</sup> (Fig. 6a). After a slight decline in the first 2 h, caspase  
470 activity increased throughout the experiment with 10 fold higher values ( $2.9 \pm 1.5$  pmol L<sup>-1</sup>  
471 mg protein<sup>-1</sup> min<sup>-1</sup>) obtained over the next 22 h as the bloom crashed (Fig. 6a).

472 We followed transcript abundance over the demise period for the 12 identified metacaspase  
473 genes in *Trichodesmium* [(Asplund-Samuelsson et al., 2012; Asplund-Samuelsson, 2015;  
474 Berman-Frank et al., 2004)]; *TeMC1* (Tery\_2077), *TeMC2* (Tery\_2689), *TeMC3* (Tery\_3869),  
475 *TeMC4* (Tery\_2471), *TeMC5* (Tery\_2760), *TeMC6* (Tery\_2058), *TeMC7* (Tery\_1841),  
476 *TeMC8* (Tery\_0382), *TeMC9* (Tery\_4625), *TeMC10* (Tery\_2624), *TeMC11* (Tery\_2158), and  
477 *TeMC12* (Tery\_2963)] (Fig. 6b, Table S1). A subset of these genes was previously implicated  
478 in PCD of *Trichodesmium* cultures in response to Fe and light stress (Bar-Zeev et al., 2013;  
479 Berman-Frank et al., 2004; Bidle, 2015). Here, we interrogated the entire suite of  
480 metacaspases in natural *Trichodesmium* populations. As the biomass crashed from T<sub>0</sub> to T<sub>22</sub>, 7  
481 out of 12 metacaspases (*TeMC1*, *TeMC3*, *TeMC4*, *TeMC7*, *TeMC8*, *TeMC9*, and *TeMC11*)  
482 were significantly upregulated 8 and 22 h after T<sub>0</sub> (Fig. 6b). For these genes, transcript  
483 abundance increased 2.3- to 5.3-fold 8 h after T<sub>0</sub> and 3.5-6.2-fold 22 h after T<sub>0</sub> (Fig. 6b, Table  
484 S1) *TeMC5* and *TeMC10* transcripts increased significantly after 22 h by 2.9- and 3.2 fold,  
485 respectively. *TeMC6* was upregulated 2.9-fold after 8 h. *TeMC2* transcripts did not  
486 significantly change over time. We did not detect any expression of *TeMC12* throughout the  
487 experiment.

488 Export flux can be enhanced by PCD-induced sinking (Bar-Zeev et al., 2013) as PCD in  
489 *Trichodesmium* results in degradation of internal components, especially gas vesicles that are  
490 required for buoyancy (Berman-Frank et al., 2004). Although we did not measure changes in  
491 buoyancy itself, we observed rapid sinking of the *Trichodesmium* biomass in the bottles and  
492 carboys. The metatranscriptomic analyses demonstrated that, excluding one copy of  
493 *gvpL/gvpF*, encoding a gas vesicle synthesis protein, gas vesicle protein (*gvp*) genes involved  
494 in gas-vesicle formation (*gvpA*, *gvpN*, *gcpK*, *gvpG* and *gvpL/gcpF*) were all significantly  
495 downregulated relative to T<sub>0</sub> (Fig. 7, Table S1).

## 496 **4 Discussion**

### 497 **4.1. Mortality processes of *Trichodesmium* – incubation results.**

#### 498 **4.1.1 Grazer and virus influence.**

499 Our microcosm incubations allowed us to specifically focus on the loss factors and show the  
500 involvement of biotic and abiotic stressors in inducing PCD and mechanistically impacting the  
501 demise and fate of a natural *Trichodesmium* bloom. We appreciate that the enclosure of the  
502 biomass in bottles and carboys may accelerate the processes occurring in the natural lagoon  
503 setting. Yet, the published rates of *Trichodesmium* mortality from field studies (Rodier and Le



504 Borgne, 2010) indicate that these can parallel our loss rates with natural bloom demise  
505 occurring 24-48 h after peak of biomass.

506 We focused initially on biotic factors that could impact the incubated *Trichodesmium* biomass.  
507 The low number of harpacticoid zooplankton specific to *Trichodesmium* (O'Neil and Roman,  
508 1994; O'Neil, 1998) in the lagoon (Hunt et al., 2016) and especially those in the bottles  
509 (personal observation) refutes the hypothesis that grazing caused the massive mortality of  
510 *Trichodesmium* biomass in our experimental incubations.

511 Viruses have been increasingly invoked as key agents terminating phytoplankton blooms  
512 (Brussaard et al., 2005; Jacquet et al., 2002; Lehahn et al., 2014; Tarutani et al., 2000; Vardi et  
513 al., 2012). In *Trichodesmium*, phages have been implicated in bloom crashes, but this  
514 mechanism has yet to be unequivocally proven (Hewson et al., 2004; Ohki, 1999); indeed, no  
515 specific *Trichodesmium* phage has been isolated or characterized to date (Brown et al., 2013).  
516 Here, total VLP abundance was highest at the time of sampling from the surface  
517 *Trichodesmium* bloom and at the start of the incubation at  $\sim 8 \times 10^6$  VLPs mL<sup>-1</sup> it actually  
518 declined 2 fold in the first eight hours of incubation before increasing over the next 32 h (Fig.  
519 4a). While our method of analysis cannot distinguish between phages infecting  
520 *Trichodesmium* from those infecting other marine bacteria, it argues against a massive, phage-  
521 induced lytic event of *Trichodesmium*. Such an event would have yielded a notable burst of  
522 VLPs upon bloom crash, especially considering the high *Trichodesmium* biomass observed.  
523 The coincidence between the maximal abundance of VLPs and highest *Trichodesmium*  
524 biomass is counter to viruses serving as the mechanism of mortality in our incubation  
525 experiments. Nonetheless, virus infection itself may be a stimulant for community N<sub>2</sub> fixation  
526 perhaps by releasing key nutrients (i.e., P or Fe) upon lysis of surrounding microbes (Weitz  
527 and Wilhelm, 2012). Although we did not characterize them here, it is indeed possible that  
528 *Trichodesmium*-specific phages were present in our incubation experiments and they may  
529 have exerted additional physiological stress on resident populations, facilitating PCD  
530 induction. Virus infection increases the cellular production of reactive oxygen species (ROS)  
531 (Evans et al., 2006; Vardi et al., 2012), which in turn can stimulate PCD in algal cells  
532 (Berman-Frank et al., 2004; Bidle, 2015; Thamatrakoln et al., 2012). Viral attack can also  
533 directly trigger PCD as part of an antiviral defense system activated to limit virus production  
534 and prevent massive viral infection (Bidle and Falkowski, 2004; Bidle, 2015; Georgiou et al.,  
535 1998).

536

#### 537 **4.1.2 Stressors impacting mortality.**

538 Nutrient stress can be acute or chronic to which organisms may acclimate on different time  
539 scales. Thus, for example, the consistently low DIP concentrations measured in the lagoon  
540 during the 22 days preceding the *Trichodesmium* surface bloom probably enabled acclimation  
541 responses such as induction of APA and other P acquisition systems. *Trichodesmium* has the  
542 ability to obtain P via inorganic and organic sources including methylphosphonate,  
543 ethylphosphonate, 2-aminoethylphosphonate (Beverdorf et al., 2010; Dyhrman et al., 2006),  
544 and via a phosphite uptake system (PtxABC) that accesses P via the reduced inorganic  
545 compound phosphite (Martínez et al., 2012; Polyviou et al., 2015). Our metatranscriptomic  
546 data demonstrated upregulated expression of genes related to all three of these uptake systems  
547 (DIP, phosphonates, phosphites) 8 and 22 h after incubation began, accompanying biomass  
548 demise (Fig. 5a). This included one gene for phosphite uptake (*ptxA*) and several genes from  
549 the phosphonate uptake operon (*phnDCEEGHIJKLM*) (Hove-Jensen et al., 2014).  
550 Upregulated expression of *phnD*, *phnC*, *phnE*, *phnH*, *phnI*, *phnJ*, *phnK*, *phnL* and *phnM*  
551 occurred as the *Trichodesmium* biomass crashed (Fig. 5a, Table S1), consistent with previous  
552 results demonstrating that *phnD* and *phnJ* expression levels increased during DIP depletion  
553 (Hove-Jensen et al., 2014). It is likely that during bloom demise, the C-P lyase pathway of  
554 remaining living cells was induced when DIP sources were extremely low, while POP and  
555 DOP increased along with the decaying organic matter. The ability to use phosphonates or  
556 phosphites as a P source can provide a competitive advantage for phytoplankton and bacteria  
557 in P-depleted waters (Coleman and Chisholm, 2010; Martinez et al., 2010). Thus, it is  
558 puzzling why dying cells would upregulate *phn* genes or *phoA* transcripts after 22 h incubation  
559 (Fig. 5a). A more detailed temporal resolution of the metatranscriptomic analyses may  
560 elucidate the expression dynamics of these genes and their regulating factors. Alternatively, in  
561 PCD-induced populations, a small percentage remains viable and resistant as either cysts  
562 (Vardi et al., 1999) or hormogonia (Berman-Frank et al., 2004) that can serve as the inoculum  
563 for future blooms. It is plausible that the observed upregulation signal was attributable to these  
564 sub-populations.

565 The concentrations of dissolved and bioavailable Fe were not measured in the lagoon water  
566 during the experimental period as Fe is typically replete in the lagoon (Jacquet et al., 2006).  
567 However, even in Fe-replete environments such as the New Caledonian lagoon, dense patches  
568 of cyanobacterial or algal biomass can deplete available resources and cause limited micro-  
569 environments (Shaked, 2002). We obtained evidence for Fe stress using several proxy genes

570 demonstrating that enhanced cellular Fe demand occurred during the bloom crash (Table S1).  
571 *Trichodesmium*'s strategies of obtaining and maintaining sufficient Fe involves genes such as  
572 *isiB*. *isiB* was highly expressed when biomass accumulated on the surface waters, indicative  
573 for higher Fe demand at this biomass load (Bar-Zeev et al., 2013; Chappell and Webb, 2010).  
574 Transcripts for chlorophyll-binding, Fe-stress-induced protein A (*IsiA*) increased (albeit not  
575 significantly) 3-fold over 22 h of bloom demise (Fig. 5b, Table S1). In many cyanobacteria,  
576 *isiA* expression is stimulated under Fe stress (Laudenbach and Straus, 1988) and oxidative  
577 stress (Jeanjean et al., 2003) and functions to prevent high-light induced oxidative damage by  
578 increasing cyclic electron flow around the photosynthetic reaction center photosystem I  
579 (Havaux et al., 2005; Latifi et al., 2005; Michel and Pistorius, 2004). Dense surface blooms of  
580 *Trichodesmium* are exposed to high irradiance (on day 23 average PAR was 3000  $\mu\text{mol}$   
581  $\text{photons m}^{-2} \text{s}^{-1}$ ). It is possible that high Fe demand combined with the oxidative stress of the  
582 high irradiance induced the higher expression of *isiA* (Fig. 5b). As cell density and associated  
583 self-shading of *Trichodesmium* filaments decreased during bloom crash, light-induced  
584 oxidative stress is likely the principal driver for elevated *isiA* expression.

585 The gene *idiA* is another environmental Fe stress biomarker that allows acquisition and  
586 transfer of Fe through the periplasm into the cytoplasm (Chappell and Webb, 2010). In our  
587 incubation, upregulated expression of *idiA* (an ABC  $\text{Fe}^{+3}$  transporter) was evident after 8 h.  
588 This is consistent with increasing Fe-limitation, as *Trichodesmium* abundance (measured via  
589 16S rRNA gene sequencing) was still high at T<sub>6</sub> (after 6 h of incubations) (replicate 1). These  
590 findings are consistent with proteomics analyses from deplete iron (0  $\mu\text{M}$  Fe) *Trichodesmium*  
591 cultures which revealed an increase in IdiA protein expression (Snow et al., 2015). Lastly, our  
592 metatranscriptomic data highlighted a reduction in Fe storage and utilization, as the expression  
593 of Fe-rich ferritin-like DPS proteins (Castruita et al., 2006), encoded by *dpsA*, decreased  $\sim 5$   
594 fold by the time that most of the biomass had crashed (T<sub>22</sub>) (Fig. 5b, Table S1). *dpsA* was also  
595 downregulated under Fe-replete conditions in *Synechococcus* (Mackey et al., 2015), but the  
596 downregulation observed here is more likely related to *Trichodesmium* cells dying and  
597 downregulating Fe-demanding processes such as photosynthesis and N<sub>2</sub> fixation.

#### 598 **4.1.3. Programmed cell death (PCD) and markers for increased export flux.**

599 The physiological and morphological evidence of PCD in *Trichodesmium* has been previously  
600 documented in both laboratory (Bar-Zeev et al., 2013; Berman-Frank et al., 2004) and  
601 environmental cultures collected from surface waters around New Caledonia (Berman-Frank

602 et al., 2004). Here, we confirmed characteristic features of autocatalytic PCD in  
603 *Trichodesmium* such as increased caspase-specific activity (Fig. 6a), globally enhanced  
604 metacaspase expression (Fig. 6b), and decreased expression of gas vesicle maintenance (Fig.  
605 7). Metatranscriptomic snapshots interrogating expression changes in all *Trichodesmium*  
606 metacaspases (Fig. 6b) generally portrayed upregulated expression concomitant with biomass  
607 decline. Our results are consistent with previous observations that Fe-depleted PCD-induced  
608 laboratory cultures of *Trichodesmium* IMS101 had higher expression levels of *TeMC1* and  
609 *TeMC9* compared to healthy Fe-replete cultures (Bar-Zeev et al., 2013; Berman-Frank et al.,  
610 2004). To our knowledge, this is the first study examining expression levels of metacaspases  
611 in environmental *Trichodesmium* samples during a natural bloom. 11 of the 12 annotated  
612 metacaspases in *Trichodesmium* were expressed in all 3 metatranscriptomes from the surface  
613 bloom. To date, no specific function has been determined for these metacaspases in  
614 *Trichodesmium* other than their association with cellular stress and death. Efforts are  
615 underway to elucidate the specific cellular functions, regulation, and protein interactions of  
616 these *Trichodesmium* metacaspases (Pfreundt et al., 2014; Spungin et al., In prep).

617 In cultures and isolated natural populations of *Trichodesmium*, high caspase-like specific  
618 activity is correlated with the initial induction stages of PCD with activity declining as the  
619 biomass crashes (Bar-Zeev et al., 2013; Berman-Frank et al., 2004; Berman-Frank et al.,  
620 2007). Here, caspase-like activity increased with the crashing populations of *Trichodesmium*  
621 (Fig. 5a). Notably, maximal caspase activities were recorded at T<sub>23</sub>, after which most  
622 *Trichodesmium* biomass had collapsed. The high protein-normalized caspase-specific activity  
623 may be a result of a very stressed and dying sub-population of *Trichodesmium* that had not yet  
624 succumbed to PCD (Berman-Frank et al., 2004). Alternatively, the high caspase-like activity  
625 may be attributed to the large population of *Alteromonas* bacteria that were associated with  
626 the remaining detrital *Trichodesmium* biomass. However, currently, we are unaware of any  
627 publications demonstrating high cellular caspase-specific activity in clades of  $\gamma$ -  
628 Proteobacteria.

629 Gas vesicles are internal structures essential for maintaining buoyancy of *Trichodesmium*  
630 populations in the upper surface waters enabling them to vertically migrate and respond to  
631 light and nutrient requirements (Capone et al., 1997; Walsby, 1978). Mortality via PCD causes  
632 a decline in the number and size of cellular gas vesicles in *Trichodesmium* (Berman-Frank et  
633 al., 2004) and results in an enhanced vertical flux of trichomes and colonies to depth (Bar-  
634 Zeev et al., 2013). Our metatranscriptomic data supported the subcellular divestment from gas

635 vesicle production during bloom decline, as the expression of vesicle-related genes was  
636 downregulated (Fig. 7). In parallel, TEP production and concentration increased to  $> 800 \mu\text{g}$   
637  $\text{GX L}^{-1}$ , a 2-fold increase from pre-bloom periods (Fig. 1d and Fig. 4c). When nutrient uptake  
638 is limited, but  $\text{CO}_2$  and light are sufficient, uncoupling occurs between photosynthesis and  
639 growth (Berman-Frank and Dubinsky, 1999), leading to increased production of excess  
640 polysaccharides, such as TEP, and corresponding with high TEP found in bloom decline  
641 phases rather than during the increase in population density (Engel, 2000; Smetacek, 1985). In  
642 earlier studies we demonstrated that PCD-induced demise in *Trichodesmium* is characterized  
643 by an increase in excreted TEP, (Berman-Frank et al., 2007) and enhanced sinking of  
644 particulate organic matter (Bar-Zeev et al., 2013). TEP itself may be positively buoyant  
645 (Azetsu-Scott and Passow, 2004), yet its stickiness causes aggregation and clumping of cells  
646 and detritus, ultimately enhancing sinking rates of large aggregates including dying  
647 *Trichodesmium* (Bar-Zeev et al., 2013).

#### 648 **4.1.4. Changes in microbial community with *Trichodesmium* decline.**

649 In the incubations, other diazotrophic populations succeeded the declining *Trichodesmium*  
650 biomass as indicated by increasing  $\text{N}_2$  fixation rates, POC, and PON (Fig. 4b). In experiment  
651 2, based on qPCR of targeted diazotrophic phylotypes, the diazotroph community composition  
652 shifted from being dominated by *Trichodesmium* spp. and unicellular groups UCYN-A1,  
653 UCYN-A2, and UCYN-B (T0), to one dominated by diatom-diazotroph associations Het-1  
654 and Het-2 (T<sub>72</sub>) (Bonnet et al. 2016b; Turk-Kubo, personal communication). In experiment 1  
655 heterotrophic bacteria thrived and increased in abundance as the *Trichodesmium* biomass  
656 crashed (Fig. 3).

657 *Trichodesmium* colonies host a wide diversity of microorganisms including specific epibionts,  
658 viruses, bacteria, eukaryotic microorganisms and metazoans (Hewson et al., 2009; Hmelo et  
659 al., 2012; Ohki, 1999; Paerl et al., 1989; Sheridan et al., 2002; Siddiqui et al., 1992; Zehr,  
660 1995). Associated epibiont bacterial abundance in dilute and exponentially growing laboratory  
661 cultures of *Trichodesmium* is relatively limited (Spungin et al., 2014) compared to bloom  
662 conditions (Hewson et al., 2009; Hmelo et al., 2012). Proliferation of *Alteromonas* and other  
663  $\gamma$ -Proteobacteria during biomass collapse (Fig. 3) confirms their reputation as opportunistic  
664 microorganisms (Allers et al., 2008; Hewson et al., 2009; Frydenborg et al., 2014; Pichon et  
665 al., 2013). Such organisms can thrive on the influx of organic nutrient sources from the  
666 decaying *Trichodesmium* as we observed (Fig. 3). Furthermore, the increase of organic matter  
667 including TEP produced by the stressed *Trichodesmium* (Fig. 1d and Fig. 4c) probably

668 stimulated growth of these copiotrophs. Moreover, as the *Trichodesmium* biomass declined in  
669 the carboys, the high concentrations of  $\text{NH}_4^+$  ( $> 5000 \text{ nmol L}^{-1}$ ) (Fig. 4b) sustained both  
670 autotrophic and heterotrophic organisms (Berthelot et al., 2015; Bonnet et al., 2015; Bonnet  
671 et., 2016b). Thus, the increase in volumetric  $\text{N}_2$  fixation and PON that was measured in the  
672 incubation bottles right after the *Trichodesmium* crash in experiment 2 (Fig 4b) probably  
673 reflects both the enhanced activity of other diazotrophs (see above and Bonnet et al. 2016b)  
674 and resistant residual *Trichodesmium* trichomes (Berman-Frank et al. 2004) with increased  
675 cell specific  $\text{N}_2$  fixation. This scenario is consistent with the hypothesis that PCD induction  
676 and death of a fraction of the population confers favorable conditions for survival and growth  
677 of individual cells (Bidle and Falkowski, 2004).

#### 678 **4.2. Implications for the lagoon system and export flux.**

679 Phytoplankton blooms and their dense surface accumulations occur under favorable physical  
680 properties of the upper ocean (e.g. temperature, mixed-layer depth, stratification) and  
681 specifically when division rates exceed loss rates derived from grazing, viral attack, and  
682 sinking or export from the mixed layer to depth (Behrenfeld, 2014). Although physical drivers  
683 such as turbulence and mixing may scatter and dilute these dense accumulations, the rapid  
684 disappearance of biomass in large sea-surface *Trichodesmium* blooms (within 1-2 d in the  
685 lagoon waters) (Rodier and Le Bourne 2010) suggests loss of biomass by other mechanisms.  
686 The lack of *Trichodesmium* developing within the VAHINE mesocosms and the spatial-  
687 temporal variability of the surface bloom in the lagoon prohibited *in-situ* sampling of the same  
688 biomass for several days and prevented conclusions regarding *in-situ* mortality rates and  
689 export flux. Furthermore, within these dense surface populations as well as in the microcosm  
690 and carboy experiments, nutrient availability was probably extremely limited due to high  
691 demand and competition (Shaked 2002). PCD induced by Fe-depletion experiments with  
692 laboratory cultures and natural populations results in rapid biomass demise typically beginning  
693 after 24 h with  $> 90 \%$  of the biomass crashing 3 to 5 days after induction (Bar-Zeev et al.,  
694 2013; Berman-Frank et al., 2004; Berman-Frank et al., 2007). In similar experiments with P-  
695 depletion, *Trichodesmium* biomass did not crash rapidly. Rather, limitation induced colony  
696 formation and elongation of trichomes (Spungin et al., 2014) and the cultures could be  
697 sustained for another couple of weeks before biomass declined significantly (unpublished  
698 data). The responses we quantified from the dying *Trichodesmium* in the carboys and bottles  
699 (Fig. 3-7) were similar to those obtained from controlled laboratory experiments where the  
700 nutrient stressors P and Fe were validated individually. However, the rapid response here

701 probably reflects an exacerbated reaction due to the simultaneous combination of different  
702 stressors and the presence of biotic components that can compete for and utilize the organic  
703 resources (carbon, nitrogen, phosphorus) generated by the dying *Trichodesmium*. In the  
704 lagoon, production of TEP by stressed biomass combined with the degradation of gas vesicles  
705 and enhanced aggregation will cause such surface accumulations or blooms to collapse  
706 leading to rapid vertical export of newly fixed nitrogen and carbon in the ocean.

707

## 708 **5 Conclusions and implications**

709 We demonstrate that the rapid demise of a *Trichodesmium* surface bloom in New Caledonia,  
710 with the disappearance of > 90 % of the biomass within 24 h in 4.5 L bottle incubations,  
711 displayed cellular responses to P and Fe stress and was mediated by a suite of PCD genes.  
712 Virus infection and lysis did not appear to directly cause the massive biomass decline.  
713 Although virus infection may have modulated the cellular and genetic responses to enhance  
714 PCD-driven loss processes. Quorum sensing among epibionts (Hmelo et al., 2012; Van Mooy  
715 et al., 2012), allelopathic interactions, and the production of toxins by *Trichodesmium* (Guo  
716 and Tester, 1994; Kerbrat et al., 2010) are additional factors that could be important for a  
717 concerted response of the *Trichodesmium* population, yet we did not examine them here.  
718 Collectively, they would facilitate rapid collapse and loss of *Trichodesmium* populations, and  
719 possibly lead to enhanced vertical fluxes and export production, as previously demonstrated in  
720 PCD-induced laboratory cultures of *Trichodesmium* (Bar-Zeev et al., 2013). We posit that  
721 PCD induced demise, in response to concurrent cellular stressors, and facilitated by concerted  
722 gene regulation, is typical in natural *Trichodesmium* blooms and leads to a high export  
723 production rather than regeneration and recycling of biomass in the upper photic layers.

724

725

## 726 **Author contributions**

727 IBF, DS, and SB conceived and planned the study. DS, UP, HB, SB, WRH, KB and IBF  
728 participated in the experimental sampling. DS, UP, WRH, HB, FN, DAR, KB, and IBF  
729 analyzed the samples and resulting data. IBF and DS wrote the manuscript with further  
730 contributions to the manuscript by UP, WRH, SB, and KB.

731

732

733 **Acknowledgments**

734 Funding was obtained for IBF through a collaborative grant from MOST Israel and the High  
735 Council for Science and Technology (HCST)-France, and a United States-Israel Binational  
736 Science Foundation (BSF) grant (No: 2008048) to IBF and KB. This research was partially  
737 funded by the Gordon and Betty Moore Foundation through Grant GBMF3789 to KDB. The  
738 participation of IBF, DS, UP, and WRH in the VAHINE experiment was supported by the  
739 German-Israeli Research Foundation (GIF), project number 1133-13.8/2011 to IBF and  
740 WRH, and the metatranscriptome analysis by the EU project MaCuMBA (Marine  
741 Microorganisms: Cultivation Methods for Improving their Biotechnological Applications;  
742 grant agreement no: 311975) to WRH. Funding for VAHINE Experimental project was  
743 provided by the Agence Nationale de la Recherche (ANR starting grant VAHINE ANR-13-  
744 JS06-0002), INSU-LEFE-CYBER program, GOPS, IRD and M.I.O. The authors thank the  
745 captain and crew of the R/V Alis, SEOH divers service from the IRD research center of  
746 Noumea (E. Folcher, B. Bourgeois and A. Renaud) and from the Observatoire Océanologique  
747 de Villefranche-sur-mer (OOV, J.M. Grisoni), and technical service of the IRD research  
748 center of Noumea for their helpful technical support. Thanks especially to E. Rahav for his  
749 assistance throughout the New Caledonia experiment and to H. Elifantz for assistance with  
750 the 16S sequencing and data analysis. This work is in partial fulfillment of the requirements  
751 for a PhD thesis for D. Spungin at Bar-Ilan University. We thank the three reviewers whose  
752 comments helped improve the manuscript substantially.

753

754

755

756

757

758

759

760

761



762 **References**

- 763 Allers, E., Niesner, C., Wild, C., and Pernthaler, J.: Microbes enriched in seawater after  
764 addition of coral mucus, *Applied and Environmental Microbiology*, 74, 3274-3278, 2008.
- 765 Anders, S., Pyl, P. T., and Huber, W.: HTSeq—A Python framework to work with high-  
766 throughput sequencing data, *Bioinformatics*, btu638, 2014.
- 767 Asplund-Samuelsson, J., Bergman, B., and Larsson, J.: Prokaryotic caspase homologs:  
768 phylogenetic patterns and functional characteristics reveal considerable diversity, *PLOS One*,  
769 7, e49888, 2012.
- 770 Asplund-Samuelsson, J.: The art of destruction: revealing the proteolytic capacity of bacterial  
771 caspase homologs, *Molecular Microbiology*, 98, 1-6, 2015.
- 772 Azetsu-Scott, K., and Passow, U.: Ascending marine particles: Significance of transparent  
773 exopolymer particles (TEP) in the upper ocean, *Limnology and Oceanography*, 49, 741-748,  
774 2004.
- 775 Bar-Zeev, E., Avishay, I., Bidle, K. D., and Berman-Frank, I.: Programmed cell death in the  
776 marine cyanobacterium *Trichodesmium* mediates carbon and nitrogen export, *The ISME*  
777 *Journal*, 7, 2340-2348, 2013.
- 778 Behrenfeld, M. J.: Climate-mediated dance of the plankton, *Nature Climate Change*, 4, 880-  
779 887, 2014.
- 780 Bergman, B., Sandh, G., Lin, S., Larsson, J., and Carpenter, E. J.: *Trichodesmium* - a  
781 widespread marine cyanobacterium with unusual nitrogen fixation properties, *FEMS*  
782 *Microbiology Reviews*, 1-17, 10.1111/j.1574-6976.2012.00352.x., 2012.
- 783 Berman-Frank, I., and Dubinsky, Z.: Balanced growth in aquatic plants: Myth or reality?  
784 Phytoplankton use the imbalance between carbon assimilation and biomass production to their  
785 strategic advantage, *Bioscience*, 49, 29-37, 1999.
- 786 Berman-Frank, I., Cullen, J. T., Shaked, Y., Sherrell, R. M., and Falkowski, P. G.: Iron  
787 availability, cellular iron quotas, and nitrogen fixation in *Trichodesmium*, *Limnology and*  
788 *Oceanography*, 46, 1249-1260, 2001.
- 789 Berman-Frank, I., Bidle, K., Haramaty, L., and Falkowski, P. G.: The demise of the marine  
790 cyanobacterium, *Trichodesmium* spp., via an autocatalyzed cell death pathway, *Limnology*  
791 *and Oceanography*, 49, 997-1005, 2004.
- 792 Berman-Frank, I., Rosenberg, G., Levitan, O., Haramaty, L., and Mari, X.: Coupling between  
793 autocatalytic cell death and transparent exopolymeric particle production in the marine  
794 cyanobacterium *Trichodesmium*, *Environmental Microbiology*, 9, 1415-1422, 10.1111/j.1462-  
795 2920.2007.01257.x, 2007.
- 796 Berthelot, H., Moutin, T., L'Helguen, S., Leblanc, K., Hélias, S., Grosso, O., Leblond, N.,  
797 Charrière, B., and Bonnet, S.: Dinitrogen fixation and dissolved organic nitrogen fueled  
798 primary production and particulate export during the VAHINE mesocosm experiment (New  
799 Caledonia lagoon), *Biogeosciences*, 12, 4099-4112, 10.5194/bg-12-4099-2015, 2015.

800 Beversdorf, L., White, A., Björkman, K., Letelier, R., and Karl, D.: Phosphonate metabolism  
801 by *Trichodesmium* IMS101 and the production of greenhouse gases, *Limnology and*  
802 *Oceanography*, 55, 1768-1778, 2010.

803 Bidle, K. D., and Falkowski, P. G.: Cell death in planktonic, photosynthetic microorganisms,  
804 *Nature Reviews Microbiology*, 2, 643-655, 2004.

805 Bidle, K. D.: The molecular ecophysiology of programmed cell death in marine  
806 phytoplankton, *Annual Review Marine Science*, 7, 341-375, 2015.

807 Bonnet, S., Berthelot, H., Turk-Kubo, K., Fawcett, S., Rahav, E., l'Helguen, S., and Berman-  
808 Frank, I.: Dynamics of N<sub>2</sub> fixation and fate of diazotroph-derived nitrogen in a low nutrient  
809 low chlorophyll ecosystem: results from the VAHINE mesocosm experiment (New  
810 Caledonia), *Biogeosciences*, 12, 19579-19626, doi:10.5194/bg-12-19579-2015, 2015.

811 Bonnet, S., Moutin, T., Rodier, M., Grisoni, J. M., Louis, F., Folcher, E., Bourgeois, B., Boré,  
812 J. M., and Renaud, A.: Introduction to the project VAHINE: Variability of vertical and trophic  
813 transfer of diazotroph derived N in the South West Pacific, *Biogeosciences*, doi:10.5194/bg-  
814 2015-615, 2016a.

815 Bonnet, S., Berthelot, H., Turk-Kubo, K., Cornet-Barthaux, V., Fawcett, S., Berman-Frank, I.,  
816 Barani, A., Dekeazemacker, J., Benavides, M., Charrière, B., and Capone, D.: *Trichodesmium*  
817 blooms support diatom growth in the Southwest Pacific Ocean, *Limnology and*  
818 *Oceanography*, 2016b. In Press.  
819

820 Brown, J. M., LaBarre, B. A., and Hewson, I.: Characterization of *Trichodesmium*-associated  
821 viral communities in the eastern Gulf of Mexico, *FEMS Microbiology Ecology*, 84, 603-613,  
822 2013.

823 Brussaard, C. P. D., Mari, X., Van Bleijswijk, J. D. L., and Veldhuis, M. J. W.: A mesocosm  
824 study of *Phaeocystis globosa* (Prymnesiophyceae) population dynamics - II. Significance for  
825 the microbial community, *Harmful Algae*, 4, 875-893, 2005.

826 Brussaard, C. R. D.: Optimization of procedures for counting viruses by flow cytometry, *App.*  
827 *Environmental Microbiology*, 70, 1506-1513, 2003.

828 Capone, D., Burns, J., Montoya, J., Michaels, A., Subramaniam, A., and Carpenter, E.: New  
829 nitrogen input to the tropical North Atlantic Ocean by nitrogen fixation by the  
830 cyanobacterium, *Trichodesmium* spp, *Global Biogeochemical Cycles*, 19, 2004.

831 Capone, D. G., and Carpenter, E. J.: Nitrogen fixation in the marine environment, *Science*,  
832 217, 1140-1142, 1982.

833 Capone, D. G., Zehr, J. P., Paerl, H. W., Bergman, B., and Carpenter, E. J.: *Trichodesmium*, a  
834 globally significant marine cyanobacterium, *Science*, 276, 1221-1229, 1997.

835 Capone, D. G., Subramaniam, A., Montoya, J. P., Voss, M., Humborg, C., Johansen, A. M.,  
836 Siefert, R. L., and Carpenter, E. J.: An extensive bloom of the N<sub>2</sub>-fixing cyanobacterium  
837 *Trichodesmium erythraeum* in the central Arabian Sea, *Marine Ecology Progress Series*, 172,  
838 281-292, 1998.

839 Castruita, M., Saito, M., Schottel, P., Elmegreen, L., Myneni, S., Stiefel, E., and Morel, F. M.:  
840 Overexpression and characterization of an iron storage and DNA-binding Dps protein from  
841 *Trichodesmium erythraeum*, Applied and Environmental Microbiology, 72, 2918-2924, 2006.

842 Chappell, P. D., and Webb, E. A.: A molecular assessment of the iron stress response in the  
843 two phylogenetic clades of *Trichodesmium*, Environmental Microbiology, 12, 13-27,  
844 10.1111/j.1462-2920.2009.02026.x, 2010.

845 Coleman, M. L., and Chisholm, S. W.: Ecosystem-specific selection pressures revealed  
846 through comparative population genomics, Proceedings of the National Academy of Sciences,  
847 107, 18634-18639, 2010.

848 Dandonneau, Y., and Gohin, F.: Meridional and seasonal variations of the sea surface  
849 chlorophyll concentration in the southwestern tropical Pacific (14 to 32 S, 160 to 175 E), Deep  
850 Sea Research Part A. Oceanographic Research Papers, 31, 1377-1393, 1984.

851 Dowd, S. E., Callaway, T. R., Wolcott, R. D., Sun, Y., McKeehan, T., Hagevoort, R. G., and  
852 Edrington, T. S.: Evaluation of the bacterial diversity in the feces of cattle using 16S rDNA  
853 bacterial tag-encoded FLX amplicon pyrosequencing (bTEFAP), BMC microbiology, 8, 125,  
854 2008.

855 Dupouy, C., Benielli-Gary, D., Neveux, J., Dandonneau, Y., and Westberry, T. K.: An  
856 algorithm for detecting *Trichodesmium* surface blooms in the South Western Tropical Pacific,  
857 Biogeosciences, 8, 3631-3647, 10.5194/bg-8-3631-2011, 2011.

858 Dyrman, S. T., Chappell, P. D., Haley, S. T., Moffett, J. W., Orchard, E. D., Waterbury, J. B.,  
859 and Webb, E. A.: Phosphonate utilization by the globally important marine diazotroph  
860 *Trichodesmium*, Nature, 439, 68-71, 2006.

861 Edgar, R. C.: UPARSE: highly accurate OTU sequences from microbial amplicon reads,  
862 Nature Methods, 10, 996-998, 2013.

863 Engel, A.: The role of transparent exopolymer particles (TEP) in the increase in apparent  
864 particle stickiness ( $\alpha$ ) during the decline of a diatom bloom, Journal of Plankton Research,  
865 22, 485-497, 2000.

866 Evans, C., Malin, G., Mills, G. P., and Wilson, W. H.: Viral infection of *Emiliania huxleyi*  
867 (prymnesiophyceae) leads to elevated production of reactive oxygen species, Journal of  
868 Phycology, 42, 1040-1047, 2006.

869 Frydenborg, B. R., Krediet, C. J., Teplitski, M., and Ritchie, K. B.: Temperature-dependent  
870 inhibition of opportunistic vibrio pathogens by native coral commensal bacteria, Microbial  
871 Ecology, 67, 392-401, 2014.

872 Georgiou, T., Yu, Y.-T., Ekunwe, S., Buttner, M., Zuurmond, A.-M., Kraal, B., Kleanthous,  
873 C., and Snyder, L.: Specific peptide-activated proteolytic cleavage of *Escherichia coli*  
874 elongation factor Tu, Proceedings of the National Academy of Sciences, 95, 2891-2895, 1998.

875 Guo, C., and Tester, P. A.: Toxic effect of the bloom-forming *Trichodesmium* sp.  
876 (Cyanophyta) to the copepod *Acartia tonsa*, Natural Toxins, 2, 222-227, 1994.

- 877 Hamady, M., Walker, J. J., Harris, J. K., Gold, N. J., and Knight, R.: Error-correcting  
878 barcoded primers for pyrosequencing hundreds of samples in multiplex, *Nature Methods*, 5,  
879 235-237, 2008.
- 880 Havaux, M., Guedeney, G., Hagemann, M., Yeremenko, N., Matthijs, H. C., and Jeanjean, R.:  
881 The chlorophyll-binding protein IsiA is inducible by high light and protects the  
882 cyanobacterium *Synechocystis* PCC6803 from photooxidative stress, *FEBS Letters*, 579,  
883 2289-2293, 2005.
- 884 Herbland, A., Le Bouteiller, A., and Raimbault, P.: Size structure of phytoplankton biomass in  
885 the equatorial Atlantic Ocean, *Deep Sea Research Part A. Oceanographic Research Papers*, 32,  
886 819-836, 1985.
- 887 Hewson, I., Govil, S. R., Capone, D. G., Carpenter, E. J., and Fuhrman, J. A.: Evidence of  
888 *Trichodesmium* viral lysis and potential significance for biogeochemical cycling in the  
889 oligotrophic ocean, *Aquatic Microbial Ecology*, 36, 1-8, 2004.
- 890 Hewson, I., Poretsky, R. S., Dyhrman, S. T., Zielinski, B., White, A. E., Tripp, H. J., Montoya,  
891 J. P., and Zehr, J. P.: Microbial community gene expression within colonies of the diazotroph,  
892 *Trichodesmium*, from the Southwest Pacific Ocean, *ISME Journal*, 3, 1286-1300,  
893 10.1038/ismej.2009.75, 2009.
- 894 Hmelo, L. R., Van Mooy, B. A. S., and Mincer, T. J.: Characterization of bacterial epibionts  
895 on the cyanobacterium *Trichodesmium*, *Aquatic Microbial Ecology*, 67, 1-U119,  
896 10.3354/ame01571, 2012.
- 897 Holmes, R. M., Aminot, A., K erouel, R., Hooker, B. A., and Peterson, B. J.: A simple and  
898 precise method for measuring ammonium in marine and freshwater ecosystems, *Canadian*  
899 *Journal of Fisheries and Aquatic Sciences*, 56, 1801-1808, 10.1139/f99-128, 1999.
- 900 Hove-Jensen, B., Zechel, D. L., and Jochimsen, B.: Utilization of Glyphosate as Phosphate  
901 Source: Biochemistry and Genetics of Bacterial Carbon-Phosphorus Lyase, *Microbiology and*  
902 *Molecular Biology Reviews*, 78, 176-197, 2014.
- 903 Hunt, B. P. V., Bonnet, S., Berthelot, H., Conroy, B. J., Foster, R., and Pagano, M.:  
904 Contribution and pathways of diazotroph derived nitrogen to zooplankton during the VAHINE  
905 mesocosm experiment in the oligotrophic New Caledonia lagoon, *Biogeosciences*  
906 *Discussions*, doi:10.5194/bg-2015-614, 2016.
- 907 Ivars-Martinez, E., Martin-Cuadrado, A.-B., D'Auria, G., Mira, A., Ferriera, S., Johnson, J.,  
908 Friedman, R., and Rodriguez-Valera, F.: Comparative genomics of two ecotypes of the marine  
909 planktonic copiotroph *Alteromonas macleodii* suggests alternative lifestyles associated with  
910 different kinds of particulate organic matter, *The ISME Journal*, 2, 1194-1212, 2008.
- 911 Jacquet, S., Heldal, M., Iglesias-Rodriguez, D., Larsen, A., Wilson, W., and Bratbak, G.: Flow  
912 cytometric analysis of an *Emiliana huxleyi* bloom terminated by viral infection, *Aquatic*  
913 *Microbial Ecology*, 27, 111-124, 2002.
- 914 Jacquet, S., Delesalle, B., Torr ton, J.-P., and Blanchot, J.: Response of phytoplankton  
915 communities to increased anthropogenic influences (southwestern lagoon, New Caledonia),  
916 *Marine Ecology Progress Series*, 320, 65-78, 2006.

- 917 Jeanjean, R., Zuther, E., Yeremenko, N., Havaux, M., Matthijs, H. C., and Hagemann, M.: A  
918 photosystem 1 *psaFJ*-null mutant of the cyanobacterium *Synechocystis* PCC 6803 expresses  
919 the *isiAB* operon under iron replete conditions, *FEBS letters*, 549, 52-56, 2003.
- 920 Kerbrat, A.-S., Darius, H. T., Pauillac, S., Chinain, M., and Laurent, D.: Detection of  
921 ciguatoxin-like and paralysing toxins in *Trichodesmium* spp. from New Caledonia lagoon,  
922 *Marine Pollution Bulletin*, 61, 360-366, 2010.
- 923 Kopylova, E., Noé, L., and Touzet, H.: SortMeRNA: fast and accurate filtering of ribosomal  
924 RNAs in metatranscriptomic data, *Bioinformatics*, 28, 3211-3217, 2012.
- 925 Langmead, B., and Salzberg, S. L.: Fast gapped-read alignment with Bowtie 2, *Nature*  
926 *Methods*, 9, 357-359, 2012.
- 927 Latifi, A., Jeanjean, R., Lemeille, S., Havaux, M., and Zhang, C.-C.: Iron starvation leads to  
928 oxidative stress in *Anabaena* sp. strain PCC 7120, *Journal of Bacteriology*, 187, 6596-6598,  
929 2005.
- 930 Laudenbach, D. E., and Straus, N. A.: Characterization of a cyanobacterial iron stress-induced  
931 gene similar to *psbC*, *Journal of Bacteriology*, 170, 5018-5026, 1988.
- 932 Leblanc, K., Cornet, V., Caffin, M., Rodier, M., Desnues, A., Berthelot, H., Turk-Kubo, K.,  
933 and Heliou, J.: Phytoplankton community structure in the VAHINE mesocosm experiment,  
934 *Biogeosciences Discussions.*, doi:10.5194/bg-2015-605, 2016.
- 935 Lehahn, Y., Koren, I., Schatz, D., Frada, M., Sheyn, U., Boss, E., Efrati, S., Rudich, Y.,  
936 Trainic, M., and Sharoni, S.: Decoupling physical from biological processes to assess the  
937 impact of viruses on a mesoscale algal bloom, *Current Biology*, 24, 2041-2046, 2014.
- 938 Luo, Y.-W., Doney, S., Anderson, L., Benavides, M., Berman-Frank, I., Bode, A., Bonnet, S.,  
939 Boström, K., Böttjer, D., and Capone, D.: Database of diazotrophs in global ocean:  
940 abundance, biomass and nitrogen fixation rates, *Earth System Science Data*, 4, 47-73, 2012.
- 941 Mackey, K. R., Post, A. F., McIlvin, M. R., Cutter, G. A., John, S. G., and Saito, M. A.:  
942 Divergent responses of Atlantic coastal and oceanic *Synechococcus* to iron limitation,  
943 *Proceedings of the National Academy of Sciences*, 112, 9944-9949, 2015.
- 944 Martin, M.: Cutadapt removes adapter sequences from high-throughput sequencing reads,  
945 *EMBnet. Journal*, 17, pp. 10-12, 2011.
- 946 Martinez, A., Tyson, G. W., and DeLong, E. F.: Widespread known and novel phosphonate  
947 utilization pathways in marine bacteria revealed by functional screening and metagenomic  
948 analyses, *Environmental Microbiology*, 12, 222-238, 10.1111/j.1462-2920.2009.02062.x,  
949 2010.
- 950 Martínez, A., Osburne, M. S., Sharma, A. K., DeLong, E. F., and Chisholm, S. W.: Phosphite  
951 utilization by the marine picocyanobacterium *Prochlorococcus* MIT9301, *Environmental*  
952 *Microbiology*, 14, 1363-1377, 2012.
- 953 Massana, R., Murray, A. E., Preston, C. M., and DeLong, E. F.: Vertical distribution and  
954 phylogenetic characterization of marine planktonic Archaea in the Santa Barbara Channel,  
955 *Applied and Environmental Microbiology*, 63, 50-56, 1997.

- 956 Michel, K. P., and Pistorius, E. K.: Adaptation of the photosynthetic electron transport chain  
957 in cyanobacteria to iron deficiency: the function of IdiA and IsiA, *Physiologia Plantarum*, 120,  
958 36-50, 2004.
- 959 Mohr, W., Grosskopf, T., Wallace, D. W., and LaRoche, J.: Methodological underestimation  
960 of oceanic nitrogen fixation rates, *PLOS One*, 5, e12583, 2010.
- 961 Montoya, J. P., Voss, M., Kahler, P., and Capone, D. G.: A simple, high-precision, high-  
962 sensitivity tracer assay for N<sub>2</sub> fixation, *Applied and Environmental Microbiology*, 62, 986-  
963 993, 1996.
- 964 Mulholland, M. R.: The fate of nitrogen fixed by diazotrophs in the ocean, *Biogeosciences*, 4,  
965 37-51, 2007.
- 966 O'Neil, J. M., and Roman, M. R.: Ingestion of the Cyanobacterium *Trichodesmium* spp by  
967 Pelagic Harpacticoid Copepods *Macrosetella*, *Miracia* and *Oculostella*, *Hydrobiologia*, 293,  
968 235-240, 1994.
- 969 O'Neil, J. M.: The colonial cyanobacterium *Trichodesmium* as a physical and nutritional  
970 substrate for the harpacticoid copepod *Macrosetella gracilis*, *Journal of Plankton Research*,  
971 20, 43-59, 1998.
- 972 Ohki, K.: A possible role of temperate phage in the regulation of *Trichodesmium* biomass,  
973 *Bulletin de l'institute oceanographique, Monaco*, 19, 287-291, 1999.
- 974 Orchard, E., Webb, E., and Dyhrman, S.: Characterization of phosphorus-regulated genes in  
975 *Trichodesmium* spp., *The Biological Bulletin*, 205, 230-231, 2003.
- 976 Paerl, H. W., Priscu, J. C., and Brawner, D. L.: Immunochemical localization of nitrogenase in  
977 marine *Trichodesmium* aggregates: Relationship to N<sub>2</sub> fixation potential, *Applied and*  
978 *Environmental Microbiology*, 55, 2965-2975, 1989.
- 979 Passow, U., and Alldredge, A. L.: A dye binding assay for the spectrophotometric  
980 measurement of transparent exopolymer particles (TEP), *Limnology and Oceanography*, 40,  
981 1326-1335, 1995.
- 982 Pfreundt, U., Kopf, M., Belkin, N., Berman-Frank, I., and Hess, W. R.: The primary  
983 transcriptome of the marine diazotroph *Trichodesmium erythraeum* IMS101, *Scientific*  
984 *Reports*, 4, 2014.
- 985 Pfreundt, U., Van Wambeke, F., Caffin, M., Bonnet, S., and Hess, W. R.: Succession within  
986 the prokaryotic communities during the VAHINE mesocosms experiment in the New  
987 Caledonia lagoon, *Biogeosciences*, 13, 2319-2337, doi:10.5194/bg-13-2319-2016, 2016.
- 988 Pichon, D., Cudennec, B., Huchette, S., Djediat, C., Renault, T., Paillard, C., and Auzoux-  
989 Bordenave, S.: Characterization of abalone *Haliotis tuberculata*–*Vibrio harveyi* interactions in  
990 gill primary cultures, *Cytotechnology*, 65, 759-772, 2013.
- 991 Pinto, F. L., Thapper, A., Sontheim, W., and Lindblad, P.: Analysis of current and alternative  
992 phenol based RNA extraction methodologies for cyanobacteria, *BMC Molecular Biology*, 10,  
993 1, 2009.

- 994 Polyviou, D., Hitchcock, A., Baylay, A. J., Moore, C. M., and Bibby, T. S.: Phosphite  
995 utilization by the globally important marine diazotroph *Trichodesmium*, Environmental  
996 Microbiology Reports, 7, 824-830, 2015.
- 997 Pujo-Pay, M., and Raimbault, P.: Improvement of the wet-oxidation procedure for  
998 simultaneous determination of particulate organic nitrogen and phosphorus collected on filters,  
999 Marine Ecology-Progress Series, 105, 203–207, 10.3354/meps105203, 1994.
- 1000 Quast, C., Pruesse, E., Yilmaz, P., Gerken, J., Schweer, T., Yarza, P., Peplies, J., and  
1001 Glöckner, F. O.: The SILVA ribosomal RNA gene database project: improved data processing  
1002 and web-based tools, Nucleic Acids Research, 41, D590-D596, 10.1093/nar/gks1219, 2013.
- 1003 Rahav, E., Herut, B., Levi, A., Mulholland, M., and Berman-Frank, I.: Springtime contribution  
1004 of dinitrogen fixation to primary production across the Mediterranean Sea, Ocean Science, 9,  
1005 489-498, 2013.
- 1006 Rodier, M., and Le Borgne, R.: Population dynamics and environmental conditions affecting  
1007 *Trichodesmium* spp. (filamentous cyanobacteria) blooms in the south-west lagoon of New  
1008 Caledonia, Journal of Experimental Marine Biology and Ecology, 358, 20-32,  
1009 10.1016/j.jembe.2008.01.016, 2008.
- 1010 Rodier, M., and Le Borgne, R.: Population and trophic dynamics of *Trichodesmium thiebautii*  
1011 in the SE lagoon of New Caledonia. Comparison with *T. erythraeum* in the SW lagoon,  
1012 Marine Pollution Bulletin, 61, 349-359, 2010.
- 1013 Shaked, Y.: Iron redox dynamics and biogeochemical cycling in the epilimnion of Lake  
1014 Kinneret, PhD thesis, Hebrew University of Jerusalem, 2002.
- 1015 Sheridan, C. C., Steinberg, D. K., and Kling, G. W.: The microbial and metazoan community  
1016 associated with colonies of *Trichodesmium* spp.: a quantitative survey, Journal of Plankton  
1017 Research, 24, 913-922, 2002.
- 1018 Siddiqui, P. J., Bergman, B., Bjorkman, P. O., and Carpenter, E. J.: Ultrastructural and  
1019 chemical assessment of poly-beta-hydroxybutyric acid in the marine cyanobacterium  
1020 *Trichodesmium thiebautii*, FEMS Microbiology Letters, 73, 143-148, 1992.
- 1021 Smetacek, V.: Role of sinking in diatom life-history cycles: ecological, evolutionary and  
1022 geological significance, Marine Biology, 84, 239-251, 1985.
- 1023 Snow, J. T., Polyviou, D., Skipp, P., Christmas, N. A., Hitchcock, A., Geider, R., Moore, C.  
1024 M., and Bibby, T. S.: Quantifying Integrated Proteomic Responses to Iron Stress in the  
1025 Globally Important Marine Diazotroph *Trichodesmium*, PLOS One, 10, e0142626, 2015.
- 1026 Spungin, D., Berman-Frank, I., and Levitan, O.: *Trichodesmium's* strategies to alleviate  
1027 phosphorus limitation in the future acidified oceans, Environmental Microbiology, 16, 1935-  
1028 1947, 2014.
- 1029 Spungin, D., Rosenberg, G., Bidle, K. D., and Berman-Frank, I.: Metacaspases and bloom  
1030 demise in the marine cyanobacterium *Trichodesmium*, In Prep.
- 1031 Strickland, J. D. H., and Parsons, T. R.: A Practical Handbook of Seawater Analysis, Fisheries  
1032 Research Board of Canada, Ottawa, 1972.

- 1033 Tandeau de Marsac, N., and Houmard, J.: Complementary chromatic adaptation:  
1034 Physiological conditions and action spectra, in: *Methods in Enzymology*, Academic Press,  
1035 318-328, 1988.
- 1036 Tarutani, K., Nagasaki, K., and Yamaguchi, M.: Viral impacts on total abundance and clonal  
1037 composition of the harmful bloom-forming phytoplankton heterosigma akashiwo, *Applied and*  
1038 *Environmental Microbiology*, 66, 4916-4920, 2000.
- 1039 Thamatrakoln, K., Korenovska, O., Niheu, A. K., and Bidle, K. D.: Whole-genome expression  
1040 analysis reveals a role for death-related genes in stress acclimation of the diatom *Thalassiosira*  
1041 *pseudonana*, *Environmental Microbiology*, 14, 67-81, 2012.
- 1042 Turk-Kubo, K., Frank, I., Hogan, M., Desnues, A., Bonnet, S., and Zehr, J.: Diazotroph  
1043 community succession during the VAHINE mesocosms experiment (New Caledonia Lagoon),  
1044 *Biogeosciences* 12, 7435-7452, doi:10.5194/bg-12-7435-2015, 2015.
- 1045 Van Mooy, B. A., Hmelo, L. R., Sofen, L. E., Campagna, S. R., May, A. L., Dyhrman, S. T.,  
1046 Heithoff, A., Webb, E. A., Momper, L., and Mincer, T. J.: Quorum sensing control of  
1047 phosphorus acquisition in *Trichodesmium* consortia, *The ISME Journal*, 6, 422-429, 2012.
- 1048 Van Wambeke, F., Pfreundt, U., Barani, A., Berthelot, H., Moutin, T., Rodier, M., Hess, W.  
1049 R., and Bonnet, S.: Heterotrophic bacterial production and metabolic balance during the  
1050 VAHINE mesocosm experiment in the New Caledonia lagoon, *Biogeosciences Discussions*,  
1051 12, 19861-19900, doi:10.5194/bgd-12-19861-2015, 2015.
- 1052 Vardi, A., Berman-Frank, I., Rozenberg, T., Hadas, O., Kaplan, A., and Levine, A.:  
1053 Programmed cell death of the dinoflagellate *Peridinium gatunense* is mediated by CO<sub>2</sub>  
1054 limitation and oxidative stress, *Current Biology: CB*, 9, 1061-1064, 1999.
- 1055 Vardi, A., Haramaty, L., Van Mooy, B. A., Fredricks, H. F., Kimmance, S. A., Larsen, A., and  
1056 Bidle, K. D.: Host-virus dynamics and subcellular controls of cell fate in a natural  
1057 coccolithophore population, *Proceedings of the National Academy of Sciences*, 109, 19327-  
1058 19332, 2012.
- 1059 Walsby, A. F.: The properties and bouyancy providing role of gas vacuoles in *Trichodesmium*,  
1060 *British Phycological Journal*, 13, 103-116, 1978.
- 1061 Weitz, J. S., and Wilhelm, S. W.: Ocean viruses and their effects on microbial communities  
1062 and biogeochemical cycles, *F1000 Biology Reports*, 4, 17, 2012.
- 1063 Wu, Z., Jenkins, B. D., Rynearson, T. A., Dyhrman, S. T., Saito, M. A., Mercier, M., and  
1064 Whitney, L. P.: Empirical bayes analysis of sequencing-based transcriptional profiling without  
1065 replicates, *BMC Bioinformatics*, 11, 564, 2010.
- 1066 Zehr, J. P.: Nitrogen fixation in the Sea: Why Only *Trichodesmium*, in: *Molecular Ecology of*  
1067 *Aquatic Microbes*, edited by: Joint, I., NATO ASI Series, Springer-Verlag, Heidelberg, 335-  
1068 363, 1995.
- 1069
- 1070



1071 **Figure legends**

1072 **Figure 1.** Temporal dynamics of pre-bloom measurements in the lagoon waters (a) Chl *a*  
1073 concentrations ( $\mu\text{g L}^{-1}$ ), (b) Virus like particles (VLP,  $\text{mL}^{-1} \times 10^6$ ), (c)  $\text{N}_2$  fixation rates ( $\text{nmol}$   
1074  $\text{L}^{-1} \text{h}^{-1}$ ) and particulate organic nitrogen (PON,  $\mu\text{mol L}^{-1}$ ). (d) Changes in the concentrations of  
1075 transparent exopolymeric particles (TEP,  $\mu\text{g GX L}^{-1}$ ) and particulate organic carbon (POC,  
1076  $\mu\text{mol L}^{-1}$ ). Water was sampled from in the lagoon outside the VAHINE mesocosms, at 1 m  
1077 depth (surface) throughout the experimental period from day 2 to 23 ( $n=3$ ). For VLP, the  
1078 standard error for technical replicates ( $n=3$ ) was  $< 1\%$ , which is smaller than symbol size.

1079 **Figure 2.** (a-c) Dense surface blooms of *Trichodesmium* observed outside the mesocosms in  
1080 the lagoon waters on day 23 at 12:00. Photos illustrate the spatial heterogeneity of the surface  
1081 accumulations and the high density of the biomass. (d-e) To examine the mechanistic of  
1082 demise (Experiment 1), *Trichodesmium* filaments and colonies were collected by plankton net  
1083 (mesh size,  $80 \mu\text{m}$ ) from the dense surface bloom (day 23, 12:00 h; designated  $T_0$ ) and  
1084 resuspended in  $0.2 \mu\text{m}$  pore-size filtered seawater (FSW) in six 4.5 L bottles. Bottles were  
1085 incubated on-deck in running-seawater pools with ambient surface temperature ( $\sim 26 \text{ }^\circ\text{C}$ ) at 50  
1086 % of the surface irradiance. Bottles were sampled every 2-4 h for different parameters until  
1087 the biomass crashed. (f) Temporal changes in Chl *a* concentrations in the bottles from the time  
1088 of biomass collection and resuspension in the bottles until the *Trichodesmium* biomass crashed  
1089  $\sim 24$  h after the experiment began ( $n=3-6$ ). Photo c. courtesy of A. Renaud.

1090 **Figure 3.** Dynamics of microbial community abundance and diversity during *Trichodesmium*  
1091 surface bloom as obtained by 16S rRNA gene sequencing for samples collected from the  
1092 surface waters outside the mesocosms during *Trichodesmium* surface accumulation (bloom)  
1093 (short-term experiment 1). Pie charts show the changes in dominant groups during the  
1094 *Trichodesmium* bloom and crash from two replicate incubation bottles (please note,  
1095 *Oscillatoriales* consisted only of *Trichodesmium* in this experiment). The graphs below show  
1096 the respective temporal dynamics of *Trichodesmium* (gray circles) and *Alteromonas* (white  
1097 triangles), the dominant bacterial species during the incubation experiment.

1098 **Figure 4.** Short-term experiment 2 - measurements from the lagoon waters following  
1099 *Trichodesmium* bloom on day 23. (a) Virus like particles (VLP,  $\text{mL}^{-1} \times 10^6$ ) and  
1100 *Trichodesmium* abundance (trichomes  $\text{L}^{-1}$ ) derived from qPCR-based abundances of  
1101 *Trichodesmium nifH* gene copies (Bonnet et al. 2016b) based on the assumption of 100 gene-  
1102 copies per trichome (b)  $\text{N}_2$  fixation rates ( $\text{nmol L}^{-1} \text{h}^{-1}$ ), particulate organic nitrogen (PON,

1103  $\mu\text{mol L}^{-1}$ ) and ammonium concentrations ( $\text{NH}_4^+$ ,  $\mu\text{mol L}^{-1}$ ). (c) Changes in the concentrations  
1104 of transparent exopolymeric particles (TEP,  $\mu\text{g GX L}^{-1}$ ) and particulate organic carbon (POC,  
1105  $\mu\text{mol L}^{-1}$ ). For experiment 2, seawater from the surface bloom was collected 5 h after the  
1106 initial surface bloom was sighted (day 23, 17:00) by directly filling 20 L polyethylene carboys  
1107 gently to avoid destroying biomass. Bottles were placed in on-deck incubators filled with  
1108 running seawater to maintain ambient surface temperature ( $\sim 26\text{ }^\circ\text{C}$ ) and covered with neutral  
1109 screening at 50 % surface irradiance levels. For all parameters, replicates were  $n=3$ . For VLP,  
1110 the standard error for technical replicates ( $n=3$ ) was  $< 1\%$ , which is smaller than symbol size.

1111 **Figure 5.** (a) Expression of alkaline phosphatase associated genes *phoA* and *phoX* (Tery\_3467  
1112 and Tery\_3845), phosphite utilization genes *ptxA*, *ptxB* and *ptxC* (Tery\_0365- Tery\_0367),  
1113 and phosphonate utilization genes (*phn* genes, Tery\_4993, Tery\_4994, Tery\_4995,  
1114 Tery\_4996\*, Tery\_4997, Tery\_4998, Tery\_4999, Tery\_5000, Tery\_5001 Tery\_5002 and  
1115 Tery\_5003). Asterisks near locus tag numbers indicate gene duplicates. (b) Iron-related genes,  
1116 *isiB* (Tery\_1666), *isiA* (Tery\_1667), *idiA* (Tery\_3377), and ferritin DPS gene *dpsA*  
1117 (Tery\_4282). Bars represent log2 fold changes of corresponding genes at T<sub>8</sub> (8 hours after T<sub>0</sub>)  
1118 and T<sub>22</sub> (22 hours after T<sub>0</sub>) in comparison to T<sub>0</sub>. Significant expression was tested with ASC  
1119 (Wu et al., 2010) and marked with an asterisk. Black asterisks represent significant change  
1120 from T<sub>0</sub>. A gene was called differentially expressed if  $P > 0.98$  (posterior probability).

1121 **Figure 6.** (a) Dynamics of caspase-specific activity rates ( $\text{pmol L}^{-1} \text{min}^{-1}$ ) of *Trichodesmium*  
1122 in the New Caledonian lagoon during bloom accumulation and bloom demise, sampled during  
1123 experiment 1. Samples ( $n=6$ ) collected from the bloom (day 23, 12:00 T<sub>0</sub>), were incubated on-  
1124 deck in an incubator fitted with running seawater to maintain ambient surface temperature ( $\sim$   
1125  $26\text{ }^\circ\text{C}$ ). (b) Transcript accumulation of metacaspase genes in the *Trichodesmium* bloom during  
1126 the short-term incubation experiment. Metacaspase genes are *TeMC1* (Tery\_2077), *TeMC2*  
1127 (Tery\_2689), *TeMC3* (Tery\_3869), *TeMC4* (Tery\_2471), *TeMC5* (Tery\_2760), *TeMC6*  
1128 (Tery\_2058), *TeMC7* (Tery\_1841), *TeMC8* (Tery\_0382), *TeMC9* (Tery\_4625), *TeMC10*  
1129 (Tery\_2624), *TeMC11* (Tery\_2158) and *TeMC12* (Tery\_2963). Bars represent log2 fold  
1130 changes at T<sub>8</sub> (8 hours after T<sub>0</sub>) and T<sub>22</sub> (22 hours since T<sub>0</sub>) in comparison to T<sub>0</sub>. Significant  
1131 expression was tested with ASC (Wu et al., 2010) and marked with an asterisk. Black asterisks  
1132 represent significant change from T<sub>0</sub>. A gene was called differentially expressed if  $P > 0.98$   
1133 (posterior probability).

1134 **Figure 7.** Change in gas vesicle protein (*gvp*) genes as obtained from metatranscriptomic  
1135 analyses of the *Trichodesmium* bloom from peak to collapse (experiment 1). *gvpA* genes  
1136 (Tery\_2330 and Tery\_2335\*) encode the main constituent of the gas vesicles that forms the  
1137 essential core of the structure; *gvpN* (Tery\_2329 and Tery\_2334) *gvpK* (Tery\_2322), *gvpG*  
1138 (Tery\_2338) and *gvpL/gvpF* (Tery\_2339 and Tery\_2340\*) encode vesicle synthesis proteins.  
1139 Bars represent log<sub>2</sub> fold changes at T<sub>8</sub> (8 hours after T<sub>0</sub>) and T<sub>22</sub> (22 hours since T<sub>0</sub>) in  
1140 comparison to T<sub>0</sub>. Significant expression was tested with ASC (Wu et al., 2010) and marked  
1141 with an asterisk. Black asterisks represent significant change from T<sub>0</sub>. A gene was called  
1142 differentially expressed if P > 0.98 (posterior probability).

1143

1144

1145

1146

1147

1148

1149

1150

1151

1152

1153

1154

1155

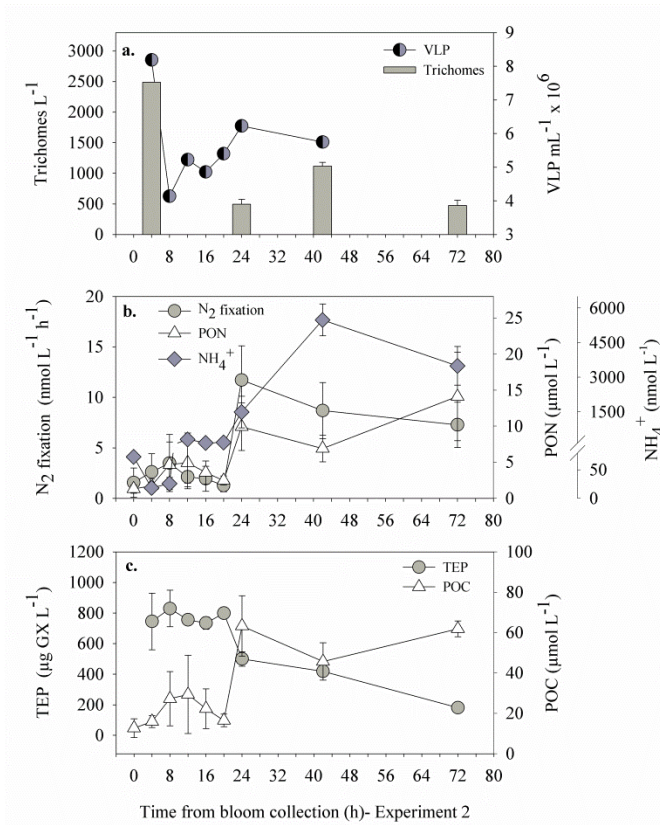
1156

1157

1158

1159

1160 **Figure 1**



1161

1162

1163

1164

1165

1166

1167

1168

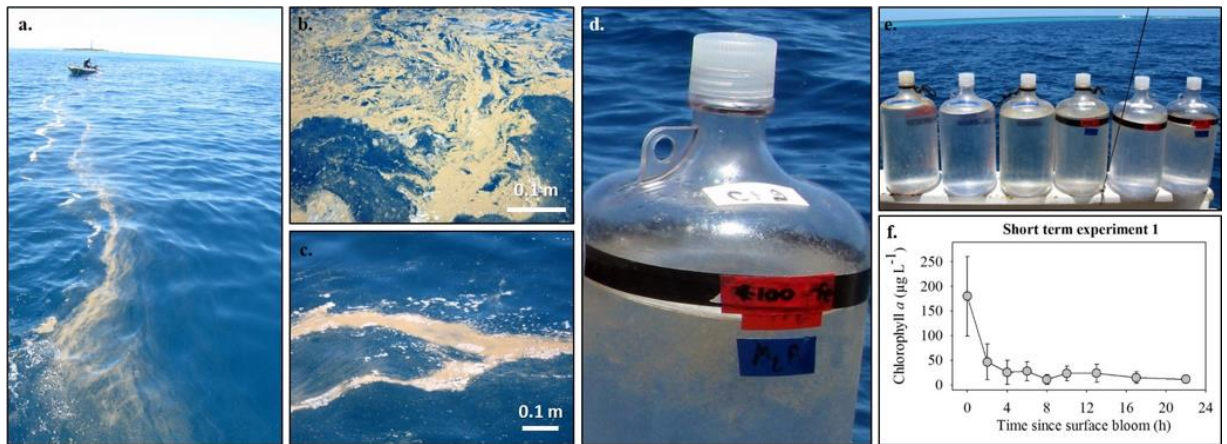
1169

1170

1171

1172

1173 **Figure 2**



1174

1175

1176

1177

1178

1179

1180

1181

1182

1183

1184

1185

1186

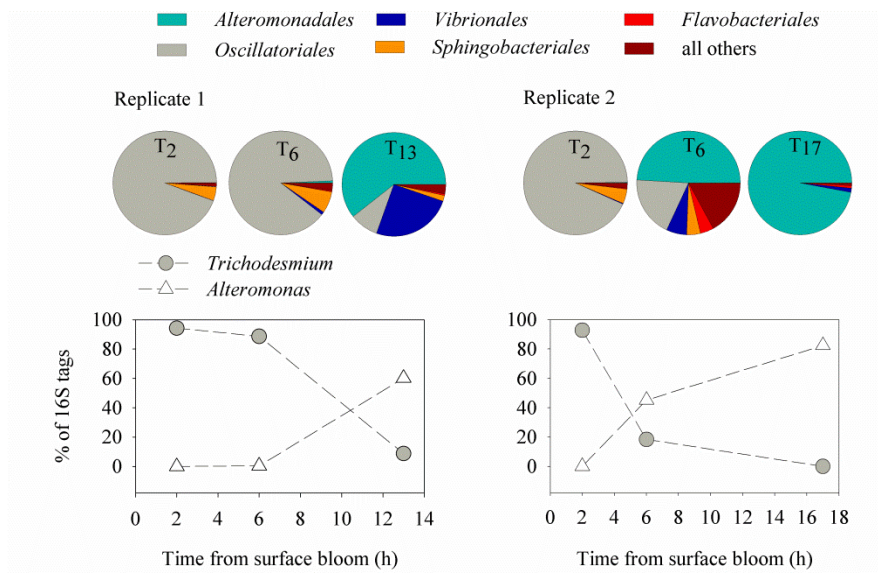
1187

1188

1189

1190

1191 **Figure 3**



1192

1193

1194

1195

1196

1197

1198

1199

1200

1201

1202

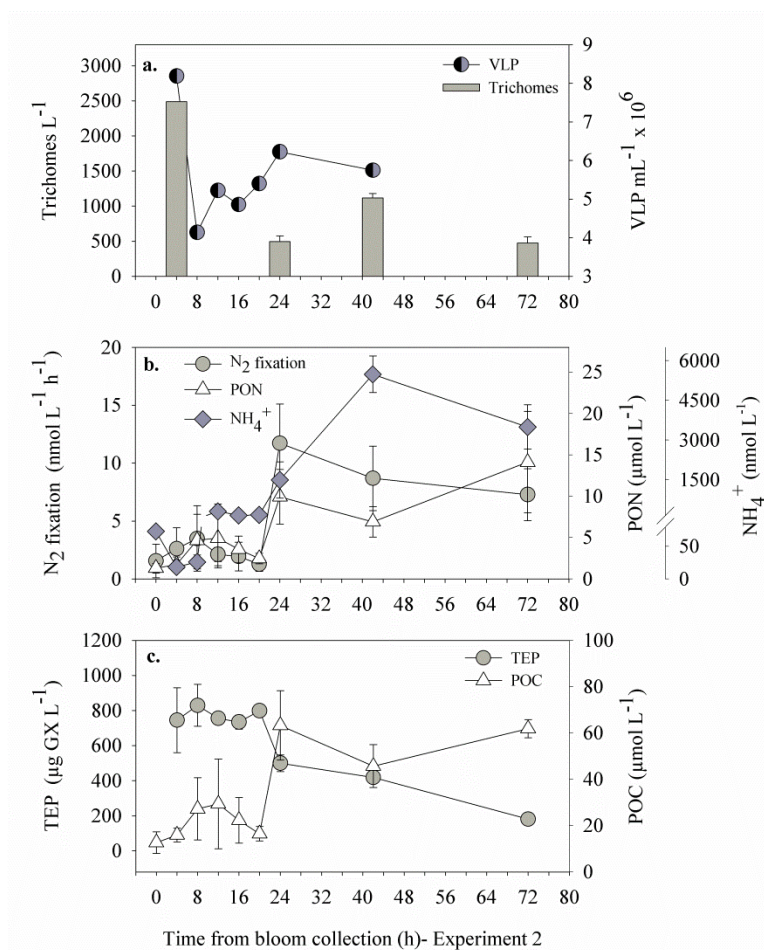
1203

1204

1205

1206

1207 **Figure 4**



1208

1209

1210

1211

1212

1213

1214

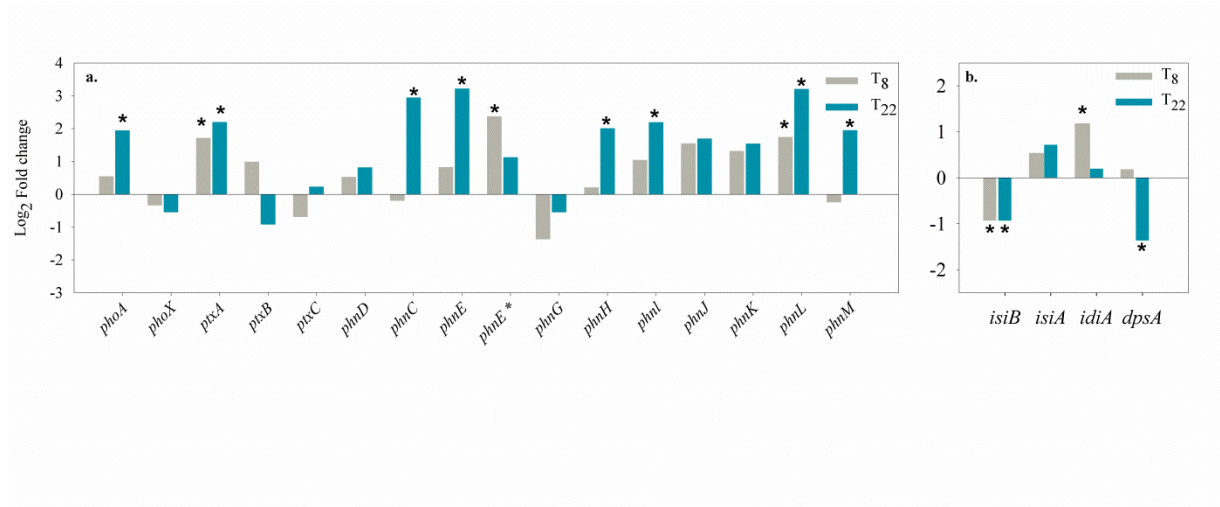
1215

1216

1217

1218

1219 **Figure 5**



1220

1221

1222

1223

1224

1225

1226

1227

1228

1229

1230

1231

1232

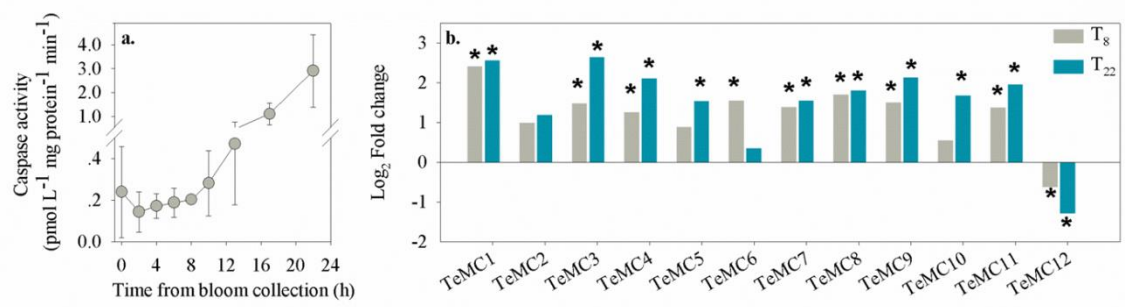
1233

1234

1235



1236 **Figure 6**



1237

1238

1239

1240

1241

1242

1243

1244

1245

1246

1247

1248

1249

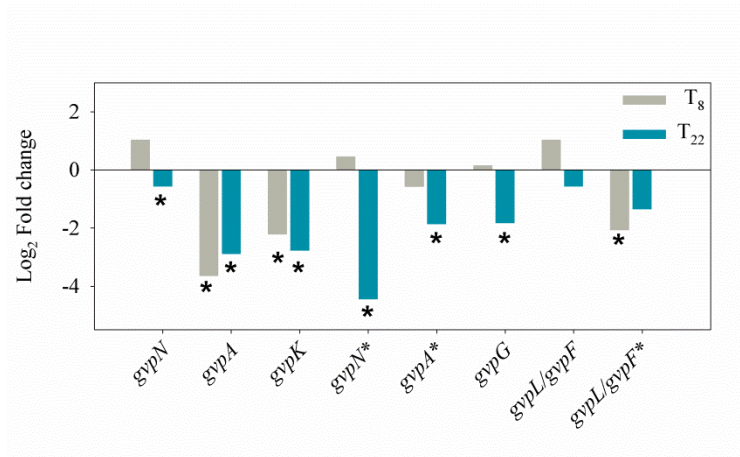
1250

1251

1252

1253

1254 **Figure 7**



1255

1256